PHILOSOPHICAL TRANSACTIONS OF THE ROYAL SOCIETY A MATHEMATICAL, PHYSICAL & ENGINEERING SCIENCES

Fluid Loading with Mean Flow. I. Response of an Elastic Plate to Localized Excitation

D. G. Crighton and J. E. Oswell

Phil. Trans. R. Soc. Lond. A 1991 **335**, 557-592
doi: 10.1098/rsta.1991.0060

Fluid loading with mean flow. I. Response of an elastic plate to localized excitation

By D. G. Crighton and J. E. Oswell

Department of Applied Mathematics and Theoretical Physics, University of Cambridge, Silver Street, Cambridge CB3 9EW, U.K.

The response to localized forcing of a fluid-loaded elastic plate is studied in the case when there is uniform incompressible flow over the plate. Absolute instability of the fluid–plate system is found when the dimensionless mean velocity U exceeds a threshold U_c which is found exactly. For $U < U_c$ the system is convectively unstable for $0 < \omega < \omega_s(U)$, neutrally stable, with anomalous features, for $\omega_s(U) < \omega < \omega_p(U)$, and stable, with conventional features, for $\omega > \omega_p(U)$, ω being the excitation frequency: here asymptotic expressions are found for the frequencies $\omega_s(U), \omega_p(U)$, and for the wavenumbers and amplitudes of the waves found upstream and downstream of the excitation. A significant feature is that $\mathrm{Re}\, A_0 < 0$ throughout $0 < \omega < \omega_p$, A_0 being the drive admittance (velocity at the point of application of the force); this means that throughout the convectively unstable and the anomalous neutral frequency ranges, the exciting force must absorb energy. An exact energy equation is derived, and shown to require the introduction of a new fluid–plate interaction flux $U\eta\phi_t$, where ϕ is the fluid potential and η the plate deflexion. The energy equation is used to illuminate properties of the convectively unstable and neutral waves, to verify the property $\mathrm{Re}\, A_0 < 0$ and to trace the waves responsible for this. Anomalous features in the frequency range $\omega_s(U) < \omega < \omega_p(U)$ are investigated further from the viewpoint of the theory of negative energy waves, and it is found that not only can some wave modes in this frequency range have negative energy, but also group velocity in an inward direction (towards the excitation). It is argued that this does not contradict the outward group velocity 'radiation condition' of M. J. Lighthill, because that condition refers expressly to circumstances in which the excitation is the sole source of all the wave energy, whereas here the excitation acts also as a scatterer, transferring energy from the mean flow to the wave field.

1. Introduction

This paper offers a contribution to the theory of wave propagation and instability in the flow of inviscid incompressible fluid over a flexible surface (in this case a thin elastic plate). Similar topics have been treated many times already in the literature, essential advances having been made by Benjamin (1960, 1963) and Landahl (1962), and with many later refinements in the modelling of the surface (with applications to stability of compliant coatings deposited on metal basic structures) and in the representation of the mean fluid velocity; see the reviews by Riley *et al.* (1988) and Gad-el-Hak (1986), and the papers by Carpenter & Garrad (1986) and Yeo & Dowling (1987). Some features of waves identified by Landahl (1962) and Benjamin (1963) have since been found to have wide applicability in wave mechanics, and the relevant

Phil. Trans. R. Soc. Lond. A (1991) **335**, 557–592
Printed in Great Britain

theory of positive and negative energy waves (PEW and NEW) has been extensively developed in plasma physics, while applications in hydrodynamic stability problems are given by Cairns (1979), Kop'ev & Leont'ev (1985) and Ostrovski *et al.* (1986).

Now most studies of waves and instabilities in fluid flow over compliant surfaces have concentrated on the propagation (downstream) of waves of specified real wavenumber, with calculation of the temporal growth rate and phase speed of such waves from the viewpoint of a classical initial value problem in which the surface deflexion $\eta(x,t)$ and velocity $\eta_t(x,t)$ are prescribed, for $-\infty < x < +\infty$, at $t = 0$. Our approach to the problem follows the rather different models in mind in the theory of *structural acoustics*. There the typical situation in mind is almost invariably one in which some source of continuous excitation is present, localized in space but simple harmonic in time. Examples include mounting points on a ship or aircraft structure that transmit local forces and moments, with time-periodic variation, arising from small out-of-balance effects in machinery (motors, pumps, gearboxes) attached to the structure at the mounting points. There is an extensive literature on the response of locally excited fluid-loaded structures in the absence of mean flow (see, for example, Cremer *et al.* 1973; Junger & Feit 1986; Fahy 1985; Crighton 1989). In these problems all wavenumbers are injected by the excitation, and one wants to understand how particular wavenumbers are filtered out as the waves develop in space at a fixed frequency. This is in general a far more difficult problem than the pure initial-value problem without continuous forcing, for it is in general possible to obtain several solutions to the single-frequency forcing problem (time dependence $\exp(-\mathrm{i}\omega t)$) and it is necessary to invoke the principle of causality to determine the unique causal one (the one – if it exists – that would arise as the long-time limit of single-frequency forcing started at some time in the distant past). Compliance with causality requires analytic variation of the solution as a function of ω throughout $\mathrm{Im}\,\omega > 0$, so that attention cannot be restricted to the single real frequency ultimately of interest and the problem becomes a global one in frequency.

Such considerations, long used in plasma instability problems, have only recently been introduced into hydrodynamic stability theory. In the book of Drazin & Reid (1981), for example, there is only a brief description of 'spatial instability' (pp. 349–353) and there is no suggestion that inversion of the dispersion relation to obtain the complex wavenumbers of waves at a prescribed single frequency needs considerations of a global kind in frequency. Moreover, the cross-stream structure of hydrodynamic instability modes is an essential feature, whereas much progress can be achieved in plasma problems with only plane-wave modes; and since the transverse hydrodynamic mode shapes and the dispersion relation $D(k,\omega) = 0$ can in almost all cases only be obtained numerically, it is hardly surprising that progress on the single-frequency response to localized forcing has been slow (except in the case of the static fluid generally studied in structural acoustics).

Recently, however, it has been increasingly recognized that many hydrodynamic stability problems should be treated as 'receptivity' problems (i.e. unstable response to localized forcing), and the causality prescription has been carried through for certain open (shear) flows; see Huerre & Monkewitz (1985) for the mixing layer problem and the same authors (1990) for a wide-ranging review. Many of the aspects of those problems, which can only be investigated numerically, and thus incompletely, can be studied in more detail in the 'basic problem of structural acoustics' (the response of a fluid-loaded structure to concentrated force excitation) with inclusion of uniform mean flow. This problem was studied by Brazier-Smith &

PHILOSOPHICAL TRANSACTIONS OF THE ROYAL SOCIETY A MATHEMATICAL, PHYSICAL & ENGINEERING SCIENCES

Scott (1984), largely through a numerical examination of the (quintic) dispersion relation, which can be obtained analytically. Brazier-Smith & Scott showed that at normalized flow speeds U exceeding a critical $U_c = 0.074$ the system was absolutely unstable, with response to any forcing initiated at some definite time diverging exponentially in time everywhere. For $U < U_c$ the system was shown to be convectively unstable for single-frequency forcing in the range $0 < \omega < \omega_s(U)$; neutrally stable, though with some anomalous features, for $\omega_s(U) < \omega < \omega_p(U)$; and stable, and behaving essentially as in the absence of mean flow, for $\omega > \omega_p(U)$. The frequencies ω_s and ω_p were determined numerically for one value of $U < U_c$.

Here we develop the study of Brazier-Smith & Scott, using exact, asymptotic and numerical methods. Asymptotic results are derived for the unstable and neutrally travelling waves and for the frequencies $\omega_s(U)$ and $\omega_p(U)$. The absolute instability threshold velocity U_c is found exactly. An expression for the drive point admittance A_0 is found for the convectively unstable case, and it reveals that $\mathrm{Re}\, A_0 < 0$, indicating a flow of energy into the driver. A study is then made of the energy flow, starting with the derivation of an exact 'energy equation'. This demands the introduction of a new flux $U\eta\phi_t$, evaluated at the plate surface, with η the deflexion, ϕ the fluctuation potential. It is shown how this energy equation is exactly satisfied by the fluxes in the wave fields at large distances and by the exact expression for $\mathrm{Re}\, A_0$, and it is found that the property $\mathrm{Re}\, A_0 < 0$ extends over the whole range $0 < \omega < \omega_p(U)$. This includes the range of anomalous neutrally stable propagation $\omega_s < \omega < \omega_p$ in which one would naturally assume a power input *from* the driver. In fact $\mathrm{Re}\, A_0 \to -\infty$ as ω approaches ω_p from below, and has a finite positive value as ω approaches ω_p from above, features predicted analytically and numerically.

In the anomalous range $\omega_s < \omega < \omega_p$, waves appear with energy flux directed towards the drive point. Although these waves may be small in amplitude compared with the convectively unstable waves (at frequencies $\omega < \omega_s$) that would inevitably have been generated in any start-up process, the energy flux in them is not, and therefore a closer look at these waves is undertaken in §5. (Here we should point out that it is shown in §4 that there is zero total flux associated with a convectively amplifying instability wave in isolation, and that any flux in the range $\omega < \omega_s$ derives from the interaction between the amplifying wave and its decaying counterpart.) Section 5 involves a discussion of the neutral waves in this system (at $\omega < \omega_s$ and $\omega_s < \omega < \omega_p$) from the theory of PEW and NEW, and shows how this theory enables propagation in the anomalous range to be understood rather better. One feature of this frequency range that is discussed in particular relates to the criterion used to avoid real-axis pole singularities in the Fourier wavenumber integral at a fixed frequency. A widely used device for this purpose was introduced by Lighthill (1960, 1978), and involves the replacement of ω by $\omega + \mathrm{i}\epsilon$, ϵ small and positive, corresponding to an excitation 'growing up' to its present value from a very low level in the distant past. Then a pole at $k = \kappa(\omega)$ for real κ is displaced for small ϵ to $k = \kappa(\omega) + \mathrm{i}\epsilon/c_g(\omega)$ with $c_g(\omega)$ the group velocity, and thus the corresponding wave mode $\exp(\mathrm{i}\kappa(\omega)\, x - \mathrm{i}\omega t)$ is picked up only in the half-space ($x > 0$ or $x < 0$) in which that mode has group velocity directed away from the excitation (localized around $x = 0$). This amounts, then, to a 'radiation condition' based on group velocity, and must give the correct causal solution provided all the energy in the wave system is delivered by the driver and provided there is no reservoir of mean energy in the system which could be tapped, and the energy converted to a wave mode, by an inhomogeneity such as a localized force.

In the present problem there is such a reservoir of energy in the mean flow, and an excitation agency that maintains a constant force $F_0 \exp(-i\omega t)$ must be prepared to dissipate or supply energy according to the phase relation between F_0 and the drive point velocity $v(0)$ which comes about in the steady-state causal solution. There is, therefore, no reason to expect the conditions for applicability of the Lighthill procedure to be met, nor is this conclusion altered by a change of reference frame to one in which the fluid at infinity is at rest, for there is then the need for dissipation or supply of energy by the agency needed to maintain the constant translation of the plate and the normal force.

Analytically this is reflected in the fact that for certain neutral wave modes $\exp(i\kappa(\omega)x - i\omega t)$ the local behaviour, for $\omega \to \omega + i\epsilon$ with ϵ small, and the global behaviour, in which ϵ can take arbitrary positive values, are found to differ. Local displacement of $\kappa(\omega)$ into the half-plane $\operatorname{Im} k < 0$ may be followed, as ϵ increases, by a return to the real axis and further displacement, eventually to infinity, in $\operatorname{Im} k > 0$. In that case the mode (with $c_g < 0$) would be picked up in $x < 0$ with outgoing group velocity if the local condition were used, but is instead picked up in $x > 0$, where it has incoming group velocity, if the global causality condition is used. Moreover, the mode in question may have positive or negative energy density, depending on a subdivision of the anomalous frequency range $[\omega_s, \omega_p]$, and thus its energy flux may be either towards or away from the excitation (here we note that the relation (energy flux) = (group velocity) × (energy density) is found to hold for neutral waves in all cases, whatever the signs of the group velocity and energy density, thereby extending the range of applicability of Lighthill's (1960, 1978) extension of Kelvin's result). It can be argued (as was mentioned a little earlier) that all these unusual features of neutral waves for $\omega_s < \omega < \omega_p$ are in fact irrelevant, because these fields are all exponentially dominated, for large x, by convectively unstable waves generated in the frequency range $0 < \omega < \omega_s$ by any physically possible start-up mechanism. That argument does not, however, apply in $x < 0$, where there are also unusual features of neutral waves, nor does it apply to the energy fluxes in the waves in $x > 0$ (the convectively amplifying waves having a flux independent of x and not necessarily dominating that of the neutral waves, as explained in §4).

We therefore think that the anomalous neutral waves may be physically significant, and argue that their appearance has to be accepted from implementation of causality arguments. The physical reason is clear; Lighthill's local group velocity condition is an analytical expression of the fact that, for the classes of system he had in mind, all the wave energy in the system is radiated away from the excitation. In our system this is not so, and all that one can say is that the forcing inhomogeneity is an energy-conversion mechanism, capable of scattering mean flow energy into wave energy without any modification to the (infinite) mean flow itself. Such conversion is not restricted to the unstable frequency range, and its ability to require the excitation to absorb energy extends beyond that range to the anomalous neutral range. Only for $\omega > \omega_p(U)$ are all the mechanisms involved described, for small U, by regular perturbations of the familiar problem of the fluid-loaded elastic plate without flow.

PHILOSOPHICAL TRANSACTIONS OF THE ROYAL SOCIETY A MATHEMATICAL, PHYSICAL & ENGINEERING SCIENCES

2. The dispersion relation

2.1. *Definition of the problem*

An infinite elastic plate of specific mass m and bending stiffness B lies in the plane $y = 0$. The half-space $y > 0$ is occupied by a fluid of density ρ_0 and sound speed c_0 moving with uniform velocity U in the positive x-direction, and there is a vacuum in $y < 0$. The plate is driven by a line forcing of magnitude $F(t)$ per unit length of the z-axis, acting in the positive y-direction and generating two-dimensional fluid motion in the (x, y) plane. We shall ultimately be interested in the time-harmonic case $F(t) = F_0 \mathrm{e}^{-\mathrm{i}\omega_0 t}$, or more strictly, in the long-time limit of the problem with $F(t) = F_0 \mathrm{e}^{-\mathrm{i}\omega_0 t} H(t)$ (H the Heaviside function), but there is a need to begin with the general time dependence. The system is at rest for $t < 0$, and $F(t) \equiv 0$ for $t < 0$.

The equations governing the system are the thin plate equation for the surface response, and velocity–displacement equation for surface velocity,

$$\left[m\frac{\partial^2}{\partial t^2} + B\frac{\partial^4}{\partial x^4}\right]\eta(x,t) = F(t)\,\delta(x) - p(x,0,t), \tag{2.1}$$

$$\frac{\partial \eta}{\partial t}(x,t) = v(x,t), \tag{2.2}$$

the kinematic boundary condition

$$\frac{\partial \phi}{\partial y}(x,0,t) = \left[\frac{\partial}{\partial t} + U\frac{\partial}{\partial x}\right]\eta(x,t), \tag{2.3}$$

the linearized Bernoulli equation relating fluid pressure and velocity potential perturbations,

$$p(x,y,t) = -\rho_0\left[\frac{\partial}{\partial t} + U\frac{\partial}{\partial x}\right]\phi(x,y,t), \tag{2.4}$$

and the wave equation

$$\left[\left(\frac{\partial}{\partial t} + U\frac{\partial}{\partial x}\right)^2 - c_0^2\nabla^2\right]\phi(x,y,t) = 0, \tag{2.5}$$

or, for incompressible flow, Laplace's equation

$$\nabla^2\phi(x,y,t) = 0. \tag{2.6}$$

The energy equation, in conservation form, for incompressible flow perturbations, is

$$\partial E/\partial t + \nabla\cdot\boldsymbol{F} = 0, \tag{2.7}$$

where the energy density E and flux $\boldsymbol{F}$ are given by

$$E = \tfrac{1}{2}\rho_0(\nabla\phi)^2, \quad \boldsymbol{F} = (p + \rho_0 U\,\partial\phi/\partial x)(\partial\phi/\partial x, \partial\phi/\partial y).$$

This follows immediately from the linearized Euler equation in the form

$$\partial\nabla\phi/\partial t + \rho_0^{-1}\nabla(p + \rho_0 U\,\partial\phi/\partial x) = 0.$$

Introducing the scalings

$$U' = (m^{\frac{3}{2}}/\rho_0 B^{\frac{1}{2}})\,U, \quad x' = (\rho_0/m)\,x, \quad t' = (\rho_0^2 B^{\frac{1}{2}}/m^{\frac{5}{2}})\,t, \quad y' = (\rho_0/m)\,y,$$
$$\phi' = (m^{\frac{1}{2}}/B^{\frac{1}{2}})\,\phi, \quad \eta' = (\rho_0/m)\,\eta, \quad v' = (m^{\frac{3}{2}}/\rho_0 B^{\frac{1}{2}})\,v, \quad p' = (m^3/\rho_0^3 B)\,p,$$
$$F'(t') = (m^2/\rho_0^2 B)\,F(t), \quad \delta(x') = (m/\rho_0)\,\delta(x), \quad c_0' = (m^{\frac{3}{2}}/\rho_0 B^{\frac{1}{2}})\,c_0,$$

we drop the $'$ and refer to equations (2.1)–(2.7) in their dimensionless forms. These are formally identical to (2.1)–(2.7) with m, B, ρ_0 replaced by unity; two independent parameters, U and c_0, remain.

We define transforms with respect to space and time as

$$\bar{\eta}(k,t) = \int_{-\infty}^{+\infty} \eta(x,t)\,\mathrm{e}^{-\mathrm{i}kx}\,\mathrm{d}x \tag{2.8}$$

and

$$\bar{\bar{\eta}}(k,\omega) = \int_{-\infty}^{+\infty} \bar{\eta}(k,t)\,\mathrm{e}^{\mathrm{i}\omega t}\,\mathrm{d}t. \tag{2.9}$$

Transform (2.8) is usually assumed to exist on the basis that all disturbances are bounded in space and decay as $|x| \to \infty$, at each finite t. However, with the thin-plate equation there is no upper limit to the propagation speed of disturbances, and these properties do not necessarily hold. For example, if the fluid is absent, then the Green's function (the solution for $\eta(x,t)$ when $F(t) = \delta(t)$) is $\eta(x,t) = (4\pi t)^{-\frac{1}{2}} H(t) \sin((x^2/4t) - \frac{1}{4}\pi)$ and is $O(1)$ as $|x| \to \infty$ for each $t > 0$. Nonetheless, the Fourier transform over x still exists because of the rapid oscillations as $|x| \to \infty$, and we assume that (2.8) always exists on the same grounds. Causality requires no response for $t < 0$ if the forcing started at $t = 0$, and (2.9) then exists subject to convergence as $t \to +\infty$. With instabilities (of maximum temporal growth rate ϵ) present in the system there is convergence only if $\operatorname{Im}\omega \equiv \omega_\mathrm{i} > \epsilon$. This condition may introduce complications when we invert the transforms.

The solution in terms of the surface displacement is

$$\eta(x,t) = \frac{1}{4\pi^2} \int_{-\infty+\mathrm{i}\omega_\mathrm{i}}^{+\infty+\mathrm{i}\omega_\mathrm{i}} \Psi(x,\omega)\,\bar{F}(\omega)\,\mathrm{e}^{-\mathrm{i}\omega t}\,\mathrm{d}\omega, \tag{2.10}$$

$$\Psi(x,\omega) = \int_c \frac{\mathrm{e}^{\mathrm{i}kx}}{D(k,\omega)}\,\mathrm{d}k. \tag{2.11}$$

Here

$$D(k,\omega) = (k^4 - \omega^2) - (\omega - Uk)^2/\gamma(k) \tag{2.12}$$

is the dispersion function and c is the k-contour running along the real axis. The function $\gamma(k) = [k^2 - (\omega - Uk)^2/c_0^2]^{\frac{1}{2}}$ has branch points in the k-plane and the cuts are fixed by taking $\operatorname{Re}\gamma > 0$ everywhere in the k-plane. As $c_0 \to \infty$ the fluid becomes incompressible, and in this paper we shall concentrate on this case. Then the branch points approach $k = 0$, and the cuts must be taken up the imaginary k-axis, from $\pm\mathrm{i}0$ to $\pm\mathrm{i}\infty$. We rewrite $D(k,\omega)$ in terms of two quintic polynomials $P_\pm(k)$, as

$$D(k,\omega) = (k^5 \mp U^2 k^2 - (\omega^2 \mp 2U\omega)\,k \mp \omega^2)/k \equiv P_\pm(k)/k, \quad \operatorname{Re} k \gtrless 0. \tag{2.13}$$

To determine the surface response for real frequencies, and thereby to get the response to single-frequency forcing, we require an analytic continuation of $\Psi(x,\omega)$ as $\omega_\mathrm{i} \to 0$. The integrand for Ψ has poles in the k-plane at appropriate roots of $P_+ P_-$,

and as ω_i is reduced from values greater than ϵ towards zero, the poles move in the k-plane. For Ψ to be analytic in ω the contour c must not be crossed by any pole as ω_i is decreased, and may therefore have to be deformed off the real axis.

2.2. *Brazier-Smith & Scott method, and results for poles*

Brazier-Smith & Scott (1984) use numerical methods to determine the loci of the roots of P_+P_-. They are found with U fixed, for a single value of $\mathrm{Re}\,\omega \equiv \omega_r$, as ω_i is reduced from a large value to zero. The process is repeated to cover a wide range of ω_r; wide enough that all interesting behaviour is said to be picked up. In this way the loci are determined, and are described in the paper by Brazier-Smith & Scott, for $U = 5$ and $\omega_r = 3.2, 3.25, 3.3$, and for two other values of U.

The roots of interest are those which will correspond to waves contributing to the surface response. In §2.1, P_+ and P_- are defined in the half planes $\mathrm{Re}\,k > 0$, $\mathrm{Re}\,k < 0$, respectively. We therefore define a valid root to be one whose path in the k-plane finishes (as $\omega_i \to 0$) in the region in which the generating polynomial is valid. A valid root is a pole of $1/D(k,\omega)$, and with $\mathrm{Im}\,k = 0$ generates a neutrally stable travelling wave in the response. For roots above the (deformed) k-contour with $\mathrm{Im}\,k \lessgtr 0$ we find corresponding exponentially growing or decaying waves respectively in the region $x > 0$, and vice versa for roots below the contour, these producing wave fields in $x < 0$. Non-valid roots give contributions bound up with those of the branch cuts, and of no distinct physical significance.

If two valid roots from different sides of the k-contour become equal, then the contour becomes 'pinched' between them. If the pinch occurs for some ω_p such that $\mathrm{Im}\,\omega_p > 0$, then the ω-contour cannot be taken completely down to the real ω-axis, and the frequency ω_p corresponds to a branch point in the ω-plane. The function $\Psi(x,\omega)$ cannot then be analytically continued as ω_i tends to zero and we cannot obtain a representation of $\Psi(x,t)$ as a Fourier integral over purely real frequencies. The response is dominated by the complex frequency ω_p, and corresponding wavenumber k_p, and the system is absolutely unstable. The integral round the branch line running downward from ω_p is dominated by a term of the form $t^{-\frac{1}{2}}\exp(-\mathrm{i}\omega_p t + \mathrm{i}k_p x)$, representing exponential growth everywhere in time. Thus if $\mathrm{Im}\,\omega_p > 0$ there is no steady state response to single-frequency forcing started at some time in the distant past. If the pinch occurs with $\mathrm{Im}\,\omega_p = 0$ then the ω-contour runs just above the real branch point ω_p, and absolute instability is avoided.

Now the function P_- has one valid root (1), which, according to Brazier-Smith & Scott, originates in the lower left-hand quadrant and moves up onto the negative real axis as $\omega_i \to 0$. The k-contour runs above this root and the wave generated is an upstream neutral travelling wave. The results for P_- are qualitatively the same for all U, and all $\omega_r > 0$. Expressions will be given later for the wavenumber $k = k_3^-$, the single valid root of P_-.

The situation with regard to P_+ is much more complicated. Figure 1 gives a qualitative representation of the loci of the roots of P_+ for any U, with ω_r very small. As ω_r is increased, the behaviour of the roots depends solely upon whether U is greater than, less than, or equal to a critical value $U_c = 0.074$ (the 'absolute instability boundary').

For any $U > U_c$, roots (3) and (4) pinch the contour at ω_p with $\mathrm{Im}\,\omega_p > 0$, leading to absolute instability. Brazier-Smith & Scott demonstrate the pinch numerically for $U = 5$, for which $\omega_r = 3.25$. The velocity $U = U_c$ marks the lower limit for absolute instability; it is the highest velocity at which the pinch occurs on the real line

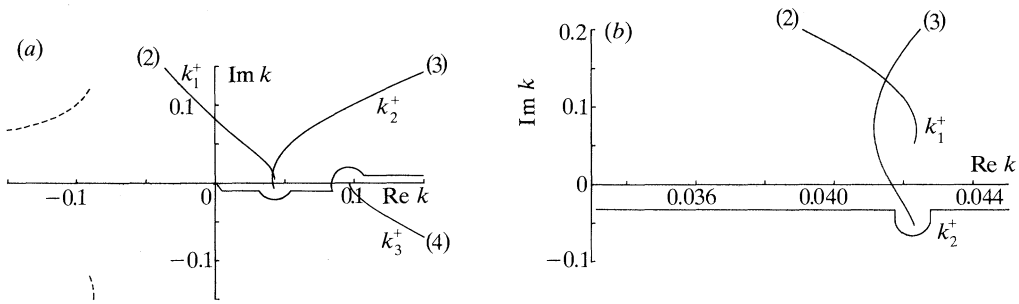

Figure 1. Loci of roots of P_+ for any U, with ω_r very small, demonstrating the typically deformed k-contour in $\mathrm{Re}\, k > 0$.

($\omega_i = 0$). For any $U < U_c$ the analytic continuation down to $\omega_i = 0$ can be completed, we have a representation of the response as an integral over all real frequencies, and we can regard $\Psi(x, \omega)$ as the causal response to single-frequency forcing at each real ω. Specifically, if $F(t) = F_0 \exp(-i\omega_0 t)$, then for $U < U_c$ the causal single-frequency response is

$$\eta(x, t) = (F_0/2\pi)\, \Psi(x, \omega_0) \exp(-i\omega_0 t). \tag{2.14}$$

It is easy to prove that, when the analytic continuation of $\Psi(x, \omega)$ down to $\omega_i = 0$ can be completed, (2.14) is indeed the long-time limit of the solution with forcing $F(t) = F_0 \exp(-i\omega_0 t) H(t)$.

In the specific case $U = 0.05 < U_c$, Brazier-Smith & Scott isolate a value $\omega_s = 0.002259$ as the upper frequency limit for spatial (convective) instability. This frequency ω_s is characterized by the merging of poles (2) and (3) on the real line. No pinch is produced; poles (2) and (3) are both above the k-contour. At a given $U < U_c$, pole (3) has $\mathrm{Im}\, k < 0$ and therefore generates a wave growing exponentially with downstream distance provided $0 < \omega < \omega_s$. Such a wave is referred to as a convective or spatial instability wave. A second frequency, $\omega_p = 0.002365$ for $U = 0.05$, is the frequency at which a pinch occurs (between (3) and (4)) on the real line. Accordingly, U_c must be the velocity at which $\omega_s = \omega_p\, (\equiv \omega_c$ say) and all three valid roots of P_+ merge; $\omega_c = 0.0047$ is the pinch frequency, determined numerically.

Details of the behaviour of the roots for $U = 5$, 0.074, 0.05 are given in Brazier-Smith & Scott (1984). We shall now determine the behaviour found by Brazier-Smith & Scott using analytical methods rather than numerical.

2.3. *Asymptotic analysis of* $P_+(k, \omega)$

Detailed analysis of $P_\pm(k, \omega)$ is unnecessary for $U > U_c\, (= 0.074)$, as we shall see that in this range the system is absolutely unstable (and in (2.24) we shall give the exact expression for U_c). Attention is therefore confined to the case $U \ll 1$, and we shall use the formal limit $U \to 0$ as the basis for asymptotics.

In turns out that there are only two distinguished scalings for ω which lead to the involvement of the mean flow in a significant (leading-order) way. These are $\omega = O(U^2)$ and $\omega = O(U^{\frac{5}{3}})$. The first of these gives results valid down to $\omega = 0$, and covers the whole of the convectively unstable range $0 < \omega < \omega_s(U)$ together with a range of frequencies above ω_s in the anomalous neutral propagation range $\omega_s(U) < \omega < \omega_p(U)$. The second gives results which overlap at the lower end with those from the first

($\omega = O(U^2)$) scaling, which complete the description of the anomalous neutral range, and which go some way beyond it, into the range $\omega > \omega_p$ in which mean flow effects are very small.

As ω increases beyond ω_p, the next distinguished scaling is found to be $\omega = O(1)$, the results for which are well known (see, for example, Crighton 1989) and describe a structure subject to heavy fluid loading by static fluid. Beyond that, for $\omega = O(U^{-\alpha})$, any $\alpha > 0$, the fluid loading becomes small and to leading order we have a vacuum dynamics problem, free of both mean flow and fluid loading effects. Since we are interested only in significant mean flow effects, we confine attention to $\omega = O(U^2)$ and $\omega = O(U^{\frac{5}{3}})$ when ω is real. Causality requires us, however, to track singularities in the k-plane as $\operatorname{Im}\omega$ decreases from large positive values to zero, and this can be done by matching a series of values of $k(\omega)$ corresponding to scalings $|\omega| = O(U^2)$, $O(U^{\frac{5}{3}})$, $O(1)$, $O(U^{-\alpha})$. Alternatively one can supplement the investigation for $\omega = O(U^2)$, $O(U^{\frac{5}{3}})$ with a limited amount of numerical work for larger $|\omega|$.

Write $\omega = U^2\Omega$ and keep $\Omega = O(1)$ as $U \to 0$. Then we find that P_+ has two roots of order U,

$$k = U\Omega \pm (U\Omega)^{\frac{3}{2}}(\Omega^2 - 1)^{\frac{1}{2}} + O(U^2), \tag{2.15}$$

these corresponding to (2) and (3) in figure 1, and three larger roots

$$k = U^{\frac{2}{3}} e^{2n\pi i/3} - \tfrac{2}{3}U\Omega - \tfrac{5}{9}U^{\frac{4}{3}}\Omega^2 e^{-2n\pi i/3} - \tfrac{70}{3^4}\Omega^3 U^{\frac{5}{3}} + O(U^2) \tag{2.16}$$

for $n = 0, 1, 2$, of which only $n = 0$ gives a valid root, corresponding to (4) in figure 1. We note that (2.15) indicates purely neutral propagation for $\Omega > 1$, approximately, and gives complex conjugate values of k for $\Omega < 1$. From the global picture given by Brazier-Smith & Scott, we may identify the upper limit for convective instability as

$$\omega_s(U) \sim U^2 \quad \text{as} \quad U \to 0. \tag{2.17}$$

This gives $\omega_s = 0.002\,500$ for the case $U = 0.05$ frequently taken by Brazier-Smith & Scott, compared with their numerically determined value 0.002 259. Calculation of some higher terms gives us a closer estimate. We find

$$k = U\Omega \pm (U\Omega)^{\frac{3}{2}}(\Omega^2 - 1)^{\frac{1}{2}} + \tfrac{1}{2}U^2(5\Omega^4 - \Omega^2) \pm \tfrac{1}{4}(U^{\frac{5}{2}}/2\Omega^{\frac{3}{2}}(\Omega^2 - 1)^{\frac{1}{2}})(5\Omega^4 - \Omega^2)^2 \pm 5U^{\frac{5}{2}}\Omega^{\frac{9}{2}}(\Omega^2 - 1)^{\frac{1}{2}} + \ldots$$

and the second and fourth terms on the right can be taken as indicating a shift of the neutral condition to

$$\Omega^2 - 1 + \tfrac{1}{4}(U/\Omega^3)(5\Omega^4 - \Omega^2)^2 = 0.$$

This gives

$$\omega_s(U) = U^2(1 - 2U + O(U^2)), \tag{2.18}$$

and for $U = 0.05$ gives $\omega_s = 0.002\,250$, with a discrepancy from 0.002 259 of exactly the order of the neglected term in (2.18).

In the range $\omega = O(U^{\frac{5}{3}})$ we put $\omega = U^{\frac{5}{3}}\Lambda$, $\Lambda = O(1)$, and find that all five roots of P_+ are $O(U^{\frac{2}{3}})$,

$$k = U^{\frac{2}{3}}\kappa_0 + \ldots \tag{2.19}$$

where

$$Q_+(\kappa_0, \Lambda) \equiv \kappa_0^5 - (\Lambda - \kappa_0)^2 = 0. \tag{2.20}$$

This quintic expression represents a balance between the plate stiffness k^4 and the fluid inertia term $(\omega - Uk)^2/k$ with inclusion of mean flow effects; only plate inertia

(ω^2) is negligible. The function Q_+ has an inflexion point at $\kappa_0 = 10^{-\frac{1}{3}}$ for all Λ, and a repeated root at $\kappa_0 = 5\Lambda/3$ for $\Lambda = \Lambda_p = (2^2 3^3/5^5)^{\frac{1}{3}}$. For $\Lambda > \Lambda_p$ it has one positive real root, and two pairs of complex conjugate roots, one pair with $\mathrm{Re}\,\kappa_0 < 0$, while for $\Lambda < \Lambda_p$ it has three real positive roots and one pair of complex conjugate roots (that pair in $\mathrm{Re}\,\kappa_0 < 0$). All this corresponds precisely to the situation described by Brazier-Smith & Scott for $\omega > \omega_p$ and $\omega_s < \omega < \omega_p$ respectively, and to leading order we therefore have the real axis pinch frequency (for which $\mathrm{d}\omega/\mathrm{d}k = 0$) as

$$\omega_p \sim U^{\frac{5}{3}} \Lambda_p, \quad \Lambda_p = N = (2^2 3^3/5^5)^{\frac{1}{3}}. \tag{2.21}$$

For $U = 0.05$ we get $\omega_p = 0.002\,210$, as compared with the computed value of $0.002\,365$. A higher approximation to the repeated root is easily found as

$$\omega_p = NU^{\frac{5}{3}}\{1 + \tfrac{5}{4}NU^{\frac{2}{3}} + O(U^{\frac{4}{3}})\} \tag{2.22}$$

and from this we get $\omega_p = 002\,332$, in good agreement with computation.

It remains to be said that the results for $\omega = O(U^2)$ are easily checked to be uniformly valid down to $\omega = 0$, and that those for $\omega = O(U^2)$ and $\omega = O(U^{\frac{5}{3}})$ match asymptotically in the overlap domain $\omega_s \ll \omega \ll \omega_p$. Further, as $|\Lambda|$ increases, the quintic $Q_+(\kappa_0, \Lambda)$ can be approximated by $\kappa_0^5 - \Lambda^2$, whose roots describe the low-frequency heavy fluid loading of the plate in static fluid. That approximation in turn fails at $\Lambda = O(U^{-\frac{5}{3}})$ ($\omega = O(1)$), where plate inertia becomes significant and comparable with the fluid inertia, but at these and all higher values of $|\omega|$ (for which indeed the fluid loading effects become completely negligible) there are no significant effects of the mean fluid flow. Note that this implies that the way in which the roots $k(\omega)$ recede to infinity as $\mathrm{Im}\,\omega$ increases to plus infinity is governed solely by the dispersion function $k^4 - \omega^2$ of the plate in vacuum. This dispersion function is not significantly changed in structure if plate damping is introduced either through a term proportional to $\partial\eta/\partial t$ or by making the bending stiffness complex with a small loss factor. The problem with damping was considered in an unpublished paper by D. Atkins mentioned by Brazier-Smith & Scott (1984) and Carpenter & Garrad (1986). Here, apparently, the system is found to be absolutely unstable for all flow speeds. However, the damping factor does not enter in a significant way and therefore the growth rate must be small, of order the damping coefficient, implying that the analysis here for zero damping must apply for many oscillation periods.

2.4. *The local behaviour of the roots*

The roots of P_+ and P_- correspond to the poles of the integrand for $\Psi(x, \omega)$, and for an analytic continuation of $\Psi(x, \omega)$ the k-contour must not be crossed by any pole. It is important to determine the paths of the roots as $\mathrm{Im}\,\omega$ is reduced from infinity to zero since it then becomes clear whether or not the contour needs to be deformed off the real axis to avoid being crossed.

Returning to the original variables, with $|\omega| \ll U^{\frac{5}{3}} \ll 1$, equations (2.15) and (2.16) yield expressions for the roots of P_+, in the convectively unstable range, as

$$k^+_{1,2} \approx \omega/U \pm \mathrm{i}(\omega/U)^{\frac{3}{2}}, \quad k^+_{n+3} \approx U^{\frac{2}{3}} \mathrm{e}^{2n\pi\mathrm{i}/3} - \tfrac{2}{3}(\omega/U) - \tfrac{5}{9}(\omega^2/U^{\frac{8}{3}})\,\mathrm{e}^{-2n\pi\mathrm{i}/3}, \quad n = 0, 1, 2. \tag{2.23}$$

Setting $\omega = \omega_r + \mathrm{i}\omega_i$ and letting ω_i increase from 0 to $o(U^{\frac{5}{3}})$ we find that the local behaviour in the k-plane is as described by figure 2.

For the paths to be fully determined we need to extend the range of the analysis to cover $O(U^{\frac{5}{3}}) \leqslant \omega_i < \infty$. Using our sequence of matched asymptotic expressions for

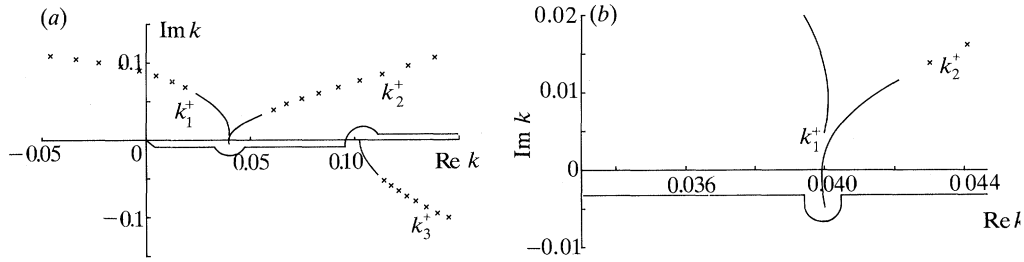

Figure 2. The local behaviour of the approximate roots of P_+ for $\omega_r = 0.002$, $U = 0.05$, ($\omega_r \ll U^{\frac{5}{3}}$) with an appropriately chosen wavenumber contour c. ——, $0 \leqslant \omega_i \leqslant U^2$; × × × ×, $U^2 \leqslant \omega_i \leqslant U^{\frac{5}{3}}$.

the roots given in §2.3 this can be done, but involves extensive algebra, and it is necessary to calculate the behaviour of the roots numerically using the full equation (cf. Brazier-Smith & Scott 1984), at least in the range $\Lambda = O(1)$; for larger Λ it is possible to again track the roots analytically. The upshot is that the local behaviour, indicated in figure 2, is representative of the global behaviour in establishing whether a pole does or does not cross the real k-axis, at least in the convectively unstable frequency range.

In this problem absolute instability will occur if either k_1^+ and k_3^+ or k_2^+ and k_3^+ merge for any $\omega_i > 0$ (k_1^+, k_2^+, k_3^+ corresponding in figure 1 to (2), (3), (4) respectively). Local analysis can be used to show that a pinch between the roots k_1^+ and k_3^+ can not occur for $\omega_i > 0$, when $U > U_c$, and thus cannot lead to absolute instability; this is produced for $U > U_c$ by a pinch between k_2^+ and k_3^+. At the critical velocity $U = U_c$, however, this pinch occurs on the real line $\omega_i = 0$, and because k_1^+ and k_2^+ are complex conjugates, it follows that for $U = U_c$, P_+ has a triple root. This phenomenon can be used to determine U_c exactly. At a triple root $P_+(k) = P'_+(k) = P''_+(k) = 0$, and solving these equations yields

$$\omega_c = (3^{\frac{1}{2}}/2^{\frac{1}{3}}5^{\frac{5}{6}})\,U_c^{\frac{5}{3}} \quad \text{where} \quad U_c = (2^{\frac{1}{2}}5^{\frac{5}{4}}/3^{\frac{3}{4}})[2-\tfrac{1}{2}(15)^{\frac{1}{2}}]^{\frac{3}{2}}. \tag{2.24}$$

The numerical values of these, $\omega_c = 0.004\,715$, $U_c = 0.074\,24$, reproduce exactly those found from computation by Brazier-Smith & Scott.

Similar asymptotic analysis can be carried out for the roots of $P_-(k, \omega)$, but the relevant results are much simpler, as P_- has only one valid root for real ω, referred to earlier as (1). For $\omega = U^2\Omega, \Omega = O(1)$ this root is

$$k_3^- = -U^{\frac{2}{3}} - \tfrac{2}{3}U\Omega + \tfrac{5}{9}U^{\frac{4}{3}}\Omega^2 - \tfrac{70}{3^4}\Omega^3 U^{\frac{5}{3}} + O(U^2), \tag{2.25}$$

and for $\omega = U^{\frac{5}{3}}\Lambda, \Lambda = O(1)$ it is

$$k_3^- = U^{\frac{2}{3}}\lambda_0 + \ldots, \tag{2.26}$$

where λ_0 is the unique real negative root of

$$Q_-(\lambda_0, \Lambda) \equiv \lambda_0^5 + (\Lambda - \lambda_0)^2 = 0. \tag{2.27}$$

These asymptotic determinations of k_3^- match as $\Omega \to \infty, \Lambda \to 0$, while (2.25) is good down to $\omega = 0$. The series (2.26) fails for large Λ, but then, as with P_+, we are back to the dominance of static fluid loading and then for still larger Λ, back to vacuum plate dynamics. From this it can be inferred, and verified by computation, that the one valid root of P_- is real and negative for real ω, and moves up from the third

quadrant onto the negative real axis as ω_i decreases from $+\infty$, all as stated by Brazier-Smith & Scott.

We must point out that the local behaviour of the roots for small positive ω_i indicates also their global behaviour for all positive ω_i only in the convectively unstable régime $\omega < \omega_s(U)$ and in the conventional stable régime $\omega > \omega_p(U)$. In the anomalous neutrally stable régime the local and global variations of the roots $k(\omega)$ may be qualitatively different. Discussion of this topic is deferred to §5.

To summarize this section, we have identified two distinct scalings, $\omega = O(U^2)$ and $\omega = O(U^{\frac{5}{3}})$, in which mean flow effects play a significant role, and we have determined asymptotic expressions for the extent $(0, \omega_s(U))$ of the convectively unstable region and for the extent $(\omega_s(U), \omega_p(U))$ of the anomalous neutrally stable region. Asymptotic expressions, as $U \to 0$, have been found for the wavenumbers of the neutral waves and the instability waves for $0 < \omega < \omega_p(U)$, and it has been shown that the wavenumbers denoted by k_1^+, k_2^+ move downwards from the upper half plane to their final positions as ω_i decreases to 0^+, while k_3^+, k_3^- move upward, from the fourth and third quadrants respectively. Accordingly, for a causal solution, the k-contour c follows the real k-axis, with an indentation above k_3^-, and above k_3^+, and with indentations below k_1^+ and k_2^+. Therefore k_3^+ and k_3^- will contribute neutral waves upstream of the excitation at $x = 0$, while k_2^+ and k_1^+ will contribute instability waves, convectively amplifying and decaying, respectively, downstream, provided $\omega < \omega_s(U)$, and will contribute neutrally stable waves downstream if $\omega_s(U) < \omega < \omega_p(U)$.

Most of the above are asymptotic results, for $U \to 0$. By contrast, the expression (2.24) for the absolute instability boundary $U = U_c$ is exact.

3. The surface response and admittances

3.1. *Introduction*

We wish to investigate the effects of the convectively unstable waves upon the system (and we shall find later that there are also unusual phenomena in the narrow frequency range $\omega_s < \omega < \omega_p$ in which there are only neutrally stable waves). We restrict attention to the region of the (ω, U) plane with $\omega \leqslant U^2$, U small, where $\omega_s \approx U^2$ is the approximate upper limit for convective instability, as determined in §2.3.

Figure 3 shows the paths taken by the roots of $D(k, \omega)$ as $\omega_i \to 0$, and the deformed contour c which yields an analytic continuation of Ψ as $\omega_i \to 0$. We have shown that the response can then be represented as an integral over real frequencies, and therefore that we can consider single-frequency forcing, $F(t) = F_0 \, e^{-i\omega_0 t}$, without further reference to initial conditions provided the deformed contour c is used. Then the transform of $F(t)$ is $\bar{F}(\omega) = 2\pi F_0 \, \delta(\omega - \omega_0)$. Using these results with (2.10) and (2.11) we determine the surface response to fixed frequency forcing as (cf. (2.14))

$$\eta(x, t) = (F_0/2\pi) \, \Psi(x, \omega_0) \exp(-i\omega_0 t), \tag{3.1}$$

where

$$\Psi(x, \omega_0) = \Psi(x, \omega)|_{\omega=\omega_0} = \int_c \frac{e^{ikx}}{D(k, \omega)} \, dk|_{\omega=\omega_0}. \tag{3.2}$$

Once Ψ is determined we obtain an explicit expression for the surface response. An exact evaluation of Ψ is possible in terms of Ei functions, but this is not helpful, and so we look for approximate solutions with x large and x small, from which we obtain the surface response in the far and near fields respectively. For brevity the suffix on ω_0 will now be dropped.

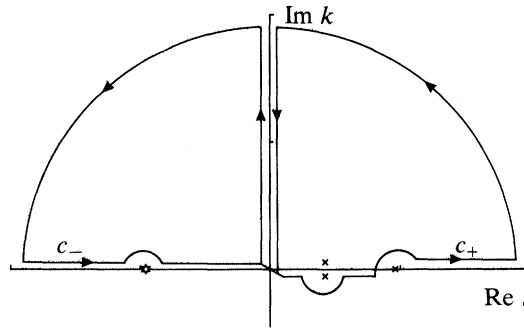

Figure 3. The roots of $D(k,\omega)$, the contours c_+, c_-, and the route taken by the completed contour when closure takes place in the upper half plane. Note that the two distinct regions of validity of $P_\pm(k)$ are separated by two branch cuts from $k = 0$.

3.2. *The far-field solutions and line transfer admittances*

There are two far fields, upstream of the drive point and downstream. We anticipate that the effect of the flow will be to produce a qualitatively different response in these regions.

We proceed with equation (2.11), which can be rewritten using (2.12) as

$$\Psi(x,\omega) = \int_{c_-(\omega)} \frac{k\,\mathrm{e}^{\mathrm{i}kx}}{P_-(k,\omega)}\,\mathrm{d}k + \int_{c_+(\omega)} \frac{k\,\mathrm{e}^{\mathrm{i}kx}}{P_+(k,\omega)}\,\mathrm{d}k, \tag{3.3}$$

where $c_-(\omega)$ and $c_+(\omega)$ are precisely the parts of $c(\omega)$ in the regions $\mathrm{Re}\,k < 0$ and $\mathrm{Re}\,k > 0$ respectively. For $0 < \omega < \omega_s$, P_+P_- has ten distinct roots, and we rewrite the above as

$$\Psi(x,\omega) = \sum_{n=1}^{5} \frac{k_n^-}{P'_-(k_n^-,\omega)} \int_{c_-(\omega)} \frac{\mathrm{e}^{\mathrm{i}kx}}{k-k_n^-}\,\mathrm{d}k + \sum_{n=1}^{5} \frac{k_n^+}{P'_+(k_n^+,\omega)} \int_{c_+(\omega)} \frac{\mathrm{e}^{\mathrm{i}kx}}{k-k_n^+}\,\mathrm{d}k. \tag{3.4}$$

With $x > 0$ (downstream) we close the contour in the upper half plane as in figure 3. The only valid poles enclosed are k_1^+ and k_2^+. The contribution from integration around the large arcs vanishes, and the branch cut contribution decays like $1/x^2$ as $|x| \to \infty$ from standard arguments. By using (2.23) for k_1^+ and k_2^+, and for simplicity taking $\Omega \ll 1$, we find (aside from the branch line contribution)

$$\eta(x,t) = (F_0/2U^{\frac{3}{2}}\omega^{\frac{1}{2}}) \exp[\mathrm{i}(\omega/U)(x-Ut)]\{\exp[(\omega/U)^{\frac{3}{2}}x] - \exp[-(\omega/U)^{\frac{3}{2}}x]\}. \tag{3.5}$$

Both waves are outgoing in phase velocity; indeed, the phase velocity is just the flow velocity. The wave generated by the pole k_1^+ decays exponentially as it propagates downstream, while that generated by k_2^+ grows with displacement from the drive point. This wave corresponds to a convective instability with spatial growth rate $(\omega/U)^{\frac{3}{2}}$, and dominates the downstream response.

With $x < 0$ (upstream) we close the contour in the lower half plane, again taking care to avoid the branch cut. The valid enclosed poles are $k_3^\pm$. Similar analysis reveals that (again aside from an algebraically decaying branch line integral)

$$\eta(x,t) = -(\mathrm{i}F_0/3U^2) \exp\{-\mathrm{i}\omega t - \tfrac{2}{3}\mathrm{i}(\omega/U)x\}[\exp(\mathrm{i}U^{\frac{2}{3}}x) - \exp-(\mathrm{i}U^{\frac{2}{3}}x)], \tag{3.6}$$

which at lowest order is a standing wave

$$\eta(x,t) = (2F_0/3U^2) \sin(U^{\frac{2}{3}}x) \exp(-\mathrm{i}\omega t),$$

but which at next order reveals upstream propagation with phase and group velocities each of magnitude $\frac{3}{2}U$ directed towards $x = -\infty$. Although this might be expected, one of the two waves in (3.6) is a negative energy wave, and therefore the corresponding energy flux is actually directed towards the excitation; see §5.

We now introduce the line transfer admittances $A^{\pm}_{\infty}$ appropriate to $x \to \pm\infty$ respectively, and defined in the convectively unstable region by

$$\left.\begin{aligned} v(x \to +\infty, t) &\equiv A^{+}_{\infty}(k^{+}_{2})\, F_0\, \mathrm{e}^{\mathrm{i}k^{+}_{2}x}\, \mathrm{e}^{-\mathrm{i}\omega t}, \\ v(x \to -\infty, t) &\equiv F_0[A^{-}_{\infty}(k^{+}_{3})\, \mathrm{e}^{\mathrm{i}k^{+}_{3}x} + A^{-}_{\infty}(k^{-}_{3})\, \mathrm{e}^{\mathrm{i}k^{-}_{3}x}]\, \mathrm{e}^{-\mathrm{i}\omega t}, \end{aligned}\right\} \tag{3.7}$$

where $v = \partial\eta/\partial t$ is the plate velocity. In the anomalous neutral propagation range $\omega_{\mathrm{s}} < \omega < \omega_{\mathrm{p}}$ the first of these has a similar additional contribution from wavenumber k^{+}_{1} and it will turn out that this must also be included in the convectively unstable region, where it decays exponentially, when the energy fluxes are calculated in §4. By using equation (2.2), which links the surface velocity and response, we can determine expressions for $A^{+}_{\infty}(k^{+}_{2}), A^{-}_{\infty}(k^{\pm}_{3})$. We find, for $\omega \ll U^2$ for example,

$$\left.\begin{aligned} A^{+}_{\infty}(k^{+}_{2}) &\equiv \omega k^{+}_{2}/P'_{+}(k^{+}_{2}) \sim -\mathrm{i}\omega^{\frac{1}{2}}/2U^{\frac{3}{2}}, \\ A^{-}_{\infty}(k^{\pm}_{3}) &\equiv -\omega k^{\pm}_{3}/P'_{\pm}(k^{\pm}_{3}) \sim \mp\omega/3U^2. \end{aligned}\right\} \tag{3.8}$$

We use these $A^{\pm}_{\infty}$ in §4 to calculate the energy fluxes in the fluid and plate in each far field.

3.3. *The near-field solution and line drive admittance*

The surface response in the near field is given by equation (3.1) in terms of the integral (3.2) with $|x|$ small. We restrict attention to the drive point ($x = 0$), for which (3.2) becomes, in the variable Λ of §2.3,

$$U^2\Psi(0,\omega) = \int_{c(\Lambda)} \frac{|\eta|}{(\eta^4 - \Lambda^2 U^{\frac{8}{3}})|\eta| - (\Lambda - \eta)^2}\, \mathrm{d}\eta$$

and since the plate inertia term is uniformly negligible when $\Lambda \leqslant O(1)$ the integral defines a function of Λ alone. This can be evaluated in elementary terms when $\Lambda \ll 1$ by dividing the deformed path $c(\Lambda)$ at $\eta = \pm A$ for arbitrary real A satisfying $\Lambda \ll A \ll 1$. Then

$$U^2\Psi(0,\omega) \sim \int^{-A}_{-\infty} \frac{\mathrm{d}\eta}{|\eta|(|\eta|^3 - 1)} - \int^{+A}_{-A} \frac{|\eta|\,\mathrm{d}\eta}{(\Lambda - \eta)^2} + \int^{+\infty}_{+A} \frac{\mathrm{d}\eta}{\eta(\eta^3 - 1)}$$

where the signs Ω, $\mho$ indicate deformation of the path above or below the relevant singularity. The first and third of these together give a real value $2\ln A + O(A^3)$, while the contribution of the middle term is $-\pi\mathrm{i} + 2 + 2\ln\Lambda - 2\ln A + O(\Lambda/A)^2$, and thus we determine

$$\Psi(0,\omega) = (1/U^2)[2 + 2\ln\Lambda - \pi\mathrm{i}], \quad \Lambda \ll 1. \tag{3.9}$$

We introduce the (dimensional) line drive admittance A_0, such that $v(0) \equiv v_0 = A_0 F_0$. The admittance A_0 is scaled according to $A'_0 = \rho_0 B^{\frac{1}{2}} A_0/m^{\frac{1}{2}}$. We drop the $'$ and refer to A_0 in its dimensionless form. A_0 is determined from equation (2.2) and the expression for the response at the drive point as

$$A_0 = -\mathrm{i}\omega\Psi(0)/2\pi = (\omega/U^2)\{-\tfrac{1}{2} - (\mathrm{i}/\pi)[1 + \ln(\omega/U^{\frac{5}{3}})]\}. \tag{3.10}$$

Now $\mathrm{Re}\, A_0$ is a measure of the power input from the forcing. The above result is unusual in that $\mathrm{Re}\, A_0 < 0$, so that the mean rate of working of the drive force is

$\frac{1}{2}|F_0|^2 \operatorname{Re} A_0 < 0$, and to maintain the postulated motion, the drive mechanism must accept and dissipate energy at the mean rate $\frac{1}{2}|F_0|^2|\operatorname{Re} A_0|$. The source of this energy must lie in the mean flow, and the excitation has provided a coupling whereby the mean flow energy can be converted into fluctuation energy in the fluid and in the plate. We shall see shortly that this property $\operatorname{Re} A_0 < 0$ extends in frequency precisely over the whole of the range $0 < \omega < \omega_p$. This range includes the frequencies $\omega_s < \omega < \omega_p$ in which the system is neutrally stable and is not confined to the range $0 < \omega < \omega_s$ in which the system is convectively unstable.

We note also that throughout the range of validity of (3.10) ($\Lambda \ll 1$), $\operatorname{Im} A_0 > 0$ and the reactive part of the drive point motion is controlled by an effective mass.

It is possible to carry out similar calculations for the high-frequency cases. For $O(1) < \Lambda < O(U^{-\frac{5}{3}})$ we approximate the denominator of the integrand for $\Psi(0, \omega)$ by

$$\eta^4|\eta| - \Lambda^2, \quad \text{for all } \eta,$$

and determine A_0 to be

$$A_0 = (1/5\omega^{\frac{1}{5}})[1 + \tfrac{2}{5}\mathrm{i}(3\sin\tfrac{4}{5}\pi - \sin\tfrac{2}{5}\pi)]. \tag{3.11}$$

For $\Lambda > O(U^{-\frac{5}{3}})$ we use the approximations

$$-\Lambda^2(U^{\frac{2}{3}}|\eta| + 1) \quad \text{for } \eta \text{ small}; \quad (\eta^4 - \Lambda^2 U^{\frac{2}{3}})|\eta| \quad \text{for } \eta \text{ large},$$

and thus for very high frequencies, with U small and fixed, we determine A_0 to first order as

$$A_0 = (1/4\omega^{\frac{1}{2}})[1 + \mathrm{i}]. \tag{3.12}$$

Thus for all $\Lambda > O(1)$ we find that $\operatorname{Re} A_0 > 0$ and the mean rate of working of the drive force is positive; as would naively be expected in a stable system (but note the result of §4, that $\operatorname{Re} A_0 < 0$ in the stable range $\omega_s < \omega < \omega_p$). We also find that $\operatorname{Im} A_0 > 0$ and this corresponds to mass dominated behaviour at the drive point at high frequencies.

We have excluded a direct calculation of A_0 for $\Lambda = O(1)$, but this case will be covered by the general results of §4.

Equations (3.11) and (3.12) correspond exactly to expressions determined for the line drive admittance by Crighton (1972). Equation (3.11), after rescaling, gives the admittance in the no-flow low-frequency or very-heavy-fluid-loading limit. Equation (3.12) is equivalent to the admittance for a line driven plate in a vacuum (no fluid loading).

4. Energy balance in the coupled fluid–plate system

4.1. *Formulation of a coupled fluid–plate energy equation*

It is possible to construct a single energy equation for the whole fluid–plate system. Multiplication of the plate equation (2.1) by the surface velocity followed by integration along the plate segment $X_1 \leqslant x \leqslant X_2$, $(y = 0)$, yields an energy equation for the plate,

$$\frac{\mathrm{d}}{\mathrm{d}t}\int_{X_1}^{X_2} \frac{1}{2}\left[\left(\frac{\partial\eta}{\partial t}\right)^2 + \left(\frac{\partial^2\eta}{\partial x^2}\right)^2\right]\mathrm{d}x = \int_{X_1}^{X_2} F\delta(x)\frac{\partial\eta}{\partial t}\,\mathrm{d}x - \int_{X_1}^{X_2} p\frac{\partial\eta}{\partial t}\,\mathrm{d}x - \left[\frac{\partial^3\eta}{\partial x^3}\frac{\partial\eta}{\partial t} - \frac{\partial^2\eta}{\partial x^2}\frac{\partial^2\eta}{\partial x\,\partial t}\right]\Bigg|_{X_1}^{X_2}. \tag{4.1}$$

The left-hand side represents the rate of increase of kinetic and potential energies in the plate. On the right we have the rate of working of the applied force, the rate of

working of the fluid pressure and the net flux of mechanical energy into the plate section $[X_1, X_2]$.

Integration of (2.7) over a volume V bounded by a surface S yields

$$\frac{\mathrm{d}}{\mathrm{d}t}\int_V \tfrac{1}{2}(\nabla\phi)^2\,\mathrm{d}V + \int_S \left(p + U\frac{\partial\phi}{\partial x}\right)\left(\frac{\partial\phi}{\partial x}, \frac{\partial\phi}{\partial y}\right)\cdot\hat{\boldsymbol{n}}\,\mathrm{d}S = 0, \tag{4.2}$$

where $\hat{\boldsymbol{n}}$ is the outward unit normal and S consists of the plate segment $X_1 \leqslant x \leqslant X_2$ with a connecting fluid surface. We may deform the fluid surface into any shape and we ensure that the most appropriate surface is chosen by examining the fluctuating field.

For all values of frequency the field consists of waves generated by the valid poles, and contributions from the branch cut integrals. The latter decay like $1/|x|^2$ and therefore carry no energy to the far fields. Waves generated by valid poles are of three types; exponentially decaying waves which do not reach the far fields; and neutral travelling waves, and exponentially growing waves both of which carry energy to the far fields across planes normal to the plate. Accordingly, we deform the surface S into a 'box' whose sides run parallel to the axes. Thus

$$\frac{\mathrm{d}}{\mathrm{d}t}\int_V \tfrac{1}{2}(\nabla\phi)^2\,\mathrm{d}V = \int_0^\infty \left(p + U\frac{\partial\phi}{\partial x}\right)\frac{\partial\phi}{\partial x}\,\mathrm{d}y\,\Big|_{x=X_1} - \int_0^\infty \left(p + U\frac{\partial\phi}{\partial x}\right)\frac{\partial\phi}{\partial x}\,\mathrm{d}y\,\Big|_{x=X_2} + \int_{X_1}^{X_2} \left(p + U\frac{\partial\phi}{\partial x}\right)\frac{\partial\phi}{\partial y}\,\mathrm{d}x\,\Big|_{y=0}. \tag{4.3}$$

All waves decay exponentially as $y \to \infty$, and therefore we have omitted from (4.3) an integral over $[X_1, X_2]$ at large y. From left to right in (4.3) we then have the rate of increase of kinetic energy in a fixed volume, and the flux of energy in the fluid (measured towards increasing x) far upstream and downstream of the drive point. The final term is the energy flux into the fluid from the surface of the plate, and substituting for $\partial\phi/\partial y$ from (2.3) and p from (2.4) we can rewrite it as

$$\int_{X_1}^{X_2} p\frac{\partial\eta}{\partial t}\,\mathrm{d}x + U\int_{X_1}^{X_2}\left(\frac{\partial\phi}{\partial x}\frac{\partial\eta}{\partial t} - \frac{\partial\phi}{\partial t}\frac{\partial\eta}{\partial x}\right)\mathrm{d}x \quad (y = 0).$$

Equations (4.1) and (4.3) now have in common a term in $p\,\partial\eta/\partial t$ and elimination of this term yields a single energy equation. We have also, however, to modify the left side of (4.3), for the energy equation must refer to the energy of the fluid in the volume actually occupied by fluid. Thus, the fluctuating energy T_f in the fluid must be defined as the quadratic approximation to

$$\int_\eta^\infty \mathrm{d}y \int_{X_1}^{X_2} \mathrm{d}x[\tfrac{1}{2}(U + \phi_x)^2 + \tfrac{1}{2}\phi_y^2 - \tfrac{1}{2}U^2],$$

which gives

$$T_\mathrm{f} = \int_0^\infty \mathrm{d}y \int_{X_1}^{X_2} \mathrm{d}x\tfrac{1}{2}(\nabla\phi)^2 - U\int_{X_1}^{X_2} \eta\phi_x(y=0)\,\mathrm{d}x, \tag{4.4}$$

and the final energy equation is

$$\frac{\mathrm{d}}{\mathrm{d}t}(T_\mathrm{f} + T_\mathrm{p} + V_\mathrm{p}) = \int_{X_1}^{X_2} F\delta(x)\frac{\partial\eta}{\partial t}\,\mathrm{d}x + (J_\mathrm{f} + J_\mathrm{p} + J_\mathrm{pf})(X_1) - (J_\mathrm{f} + J_\mathrm{p} + J_\mathrm{pf})(X_2). \tag{4.5}$$

Here

$$T_{\mathrm{p}} = \frac{1}{2}\int_{X_1}^{X_2}\left(\frac{\partial \eta}{\partial t}\right)^2 \mathrm{d}x \tag{4.6}$$

is the kinetic energy in the plate,

$$V_{\mathrm{p}} = \frac{1}{2}\int_{X_1}^{X_2}\left(\frac{\partial^2 \eta}{\partial x^2}\right)^2 \mathrm{d}x \tag{4.7}$$

is the elastic (bending) energy in the plate,

$$J_{\mathrm{f}} = \int_0^{\infty}(p + U\phi_x)\,\phi_x\,\mathrm{d}y \tag{4.8}$$

is the energy flux in the fluid across section x,

$$J_{\mathrm{p}} = \eta_{xxx}\,\eta_t - \eta_{xx}\,\eta_{xt} \tag{4.9}$$

is the mechanical energy flux in the plate across section x, and

$$J_{\mathrm{pf}} = U\eta\phi_t \tag{4.10}$$

is a coupling flux term (which we note, in contrast to the other fluxes, is not expressed in terms of locally measurable primitive variables such as p and the velocities ϕ_x, ϕ_y, but in terms of the non-local potential ϕ itself).

Although we have looked at the behaviour of the poles for complex frequency, our final solution for the response when $U < U_{\mathrm{c}}$ is a steady state solution with time dependence $\mathrm{e}^{-\mathrm{i}\omega t}$, ω real. All the instabilities are convective and grow with displacement from the drive point and not with time. Defining time averaging such that $\langle f(x,t)\,g(x,t)\rangle = \frac{1}{2}\mathrm{Re}\{f(x)\,g^*(x)\}$, we then have the steady-state energy equation in the form

$$J(X_2) = J(X_1) + I_0, \tag{4.11}$$

where

$$J(x) = J_{\mathrm{f}}(x) + J_{\mathrm{p}}(x) + J_{\mathrm{pf}}(x), \tag{4.12}$$

$$I_0 = \frac{1}{2}\int_{X_1}^{X_2}\mathrm{Re}\{F_0\,\delta(x)\,\eta_t^*\}\,\mathrm{d}x = \tfrac{1}{2}|F_0|^2\,\mathrm{Re}\,A_0, \tag{4.13}$$

and $J_{\mathrm{f}}, J_{\mathrm{p}}, J_{\mathrm{pf}}$ now refer to the time-averaged fluxes defined in (4.8)–(4.10).

The integral I_0 represents the power input into the system by the line forcing at the origin. If the plate segment is chosen such that the drive point is excluded, then $I_0 \equiv 0$. The integral J_{f} represents the flux of energy (towards increasing x) in the fluid. The flux term J_{pf} describes a coupling between the fluid potential and the surface velocity. This term is unusual in that it contains a non-primitive quantity ϕ, and we note that it is found only when there is a flow present and $U \neq 0$. It has no physical interpretation as yet, but it is significant because it indicates that there is a mechanism present by which the plate and fluid can exchange energy directly when the fluid is in bulk motion. The flux term J_{p} is standard, and represents the flux of mechanical energy in the plate. Equation (4.11) states simply that the total flux J defined by (4.12) is constant between stations X_1, X_2 if there is no energy input in that range, and increases by the mean rate of working of any external forces F_0 otherwise. The result is general, but simplifies when X_1 and X_2 lie in the far fields upstream and/or downstream of the excitation.

4.2. *Determination of the potential and pressure*

We have obtained the plate velocity as

$$v(x,t) = \begin{cases} A_0 F_0 \, \mathrm{e}^{-\mathrm{i}\omega t}, & x = 0, \\ F_0[A_\infty^+(k_1^+)\,\mathrm{e}^{\mathrm{i}k_1^+ x} + A_\infty^+(k_2^+)\,\mathrm{e}^{\mathrm{i}k_2^+ x}]\,\mathrm{e}^{-\mathrm{i}\omega t}, & x \to +\infty, \\ F_0[A_\infty^-(k_3^+)\,\mathrm{e}^{\mathrm{i}k_3^+ x} + A_\infty^-(k_3^-)\,\mathrm{e}^{\mathrm{i}k_3^- x}]\,\mathrm{e}^{-\mathrm{i}\omega t}, & x \to -\infty. \end{cases} \tag{4.14}$$

Solving Laplace's equation with decay conditions as $y \to \infty$ and using the conditions at the surface then gives the corresponding potential and pressure in the fluid. The expressions hold generally in the range $U < U_c$, in which range the roots have been shown to change their character with frequency. The surface displacement, surface velocity, fluid potential and pressure can all be determined for any frequency, using these equations together with the appropriate expressions for the roots and admittances.

4.3. *Evaluation of the energy fluxes*

The energy integral will be evaluated in the three régimes, $\omega < \omega_s$, $\omega_s < \omega < \omega_p$ and $\omega_p < \omega$, with $U < U_c$ throughout.

We begin by considering the waves downstream of the drive point. To second order, with $\omega \ll \omega_s$, the roots $k_{1,2}^+$ are given by

$$k_{1,2}^+ = \omega/U \pm \mathrm{i}(\omega/U)^{\frac{3}{2}},$$

but in what follows the results are *exact*. The lower sign root generates an exponentially growing wave which dominates the downstream far field. The upper root generates an exponentially decaying wave which fails to reach the far field. However, the energy fluxes J_f, J_p, J_{pf} must be calculated using the expressions for the pressure, velocity, etc., for both waves; cross terms appear because of the presence of two waves. The results are summarized in table 1. The net flux of energy downstream associated with the wave $(\mathrm{e}^{\mathrm{i}k_2^+ x})$ is the sum J of $J_f(k_2^+), J_p(k_2^+), J_{pf}(k_2^+)$. Each contribution is exponentially large and if we are to satisfy (4.11) with X_1, X_2 both positive ($I_0 \equiv 0$), then we anticipate $J(k_2^+, X_1) = J(k_2^+, X_2) \equiv 0$. From table 1, we determine the downstream flux associated with the growing wave $(\mathrm{e}^{\mathrm{i}k_2^+ x})$ to be (note that we use an overbar to indicate complex conjugate where necessary)

$$J(k_2^+, X_2 > 0) = \frac{|F_0|^2}{4\omega} \frac{|A_\infty^+(k_2^+)|^2}{|k_2^+|^2} \exp\left[\mathrm{i}(k_2^+ - \overline{k_2^+})\, X_2\right] \times \mathrm{Re}\left\{(\omega^2 - U^2|k_2^+|^2) + |k_2^+|^2 (k_2^+ + \overline{k_2^+})\,(k_2^{+2} + \overline{k_2^+}^2)\right\}. \tag{4.15}$$

We observe that the real part of the curly bracket is equal to

$$\mathrm{Re}\left\{\frac{|k_2^+|^2}{(k_2^+ - \overline{k_2^+})}\left[\frac{P_+(k_2^+)}{k_2^+} - \frac{P_+(\overline{k_2^+})}{\overline{k_2^+}}\right]\right\} \equiv 0,$$

and so the net flux of energy associated solely with the exponentially growing downstream wave is indeed zero, i.e.

$$J(k_2^+, X_2 > 0) \equiv 0, \quad \text{when} \quad \omega < \omega_s, \quad \text{with} \quad U < U_c. \tag{4.16}$$

A similar calculation of the flux associated solely with the decaying wave shows that this too is zero. The cross term, however, produces a net downstream flux. Using the

PHILOSOPHICAL TRANSACTIONS OF THE ROYAL SOCIETY A MATHEMATICAL, PHYSICAL & ENGINEERING SCIENCES

results $k_1^+ = \overline{k_2^+}$ and $P_+(k_{1,2}^+) = 0, \overline{P'_+(k_{1,2}^+)} = P'_+(\overline{k_{1,2}^+})$, for $\omega < \omega_s$, $U < U_c$, we substitute for $A_\infty^+(k_{1,2}^+)$ from equation (3.8) to determine

$$J(k_1^+, k_2^+, X_2 > 0) = \tfrac{1}{4}|F_0|^2 \omega \operatorname{Re}\{k_1^+/P'_+(k_1^+) + k_2^+/P'_+(k_2^+)\}.$$

The total downstream flux is given by

$$J(X_2 > 0) = J(k_1^+, X_2) + J(k_2^+, X_2) + J(k_1^+, k_2^+, X_2), \tag{4.17}$$

$$= \tfrac{1}{4}|F_0|^2 \omega \operatorname{Re}\{k_1^+/P'_+(k_1^+) + k_2^+/P'_+(k_2^+)\}, \quad \omega < \omega_s, \quad U < U_c. \tag{4.18}$$

With the frequency in the range $\omega_s < \omega < \omega_p$ the roots are given to second order by

$$k_{1,2}^+ = \omega/U \pm \omega^{\frac{5}{2}}/U^{\frac{7}{2}},$$

but again the results below are *exact* and do not use this approximation. The roots are real and unequal, and generate two outgoing stable travelling waves. Both waves are seen in the downstream far field and both are used in the calculation of the energy terms. Cross terms again appear. The results are summarized in table 1.

We begin by considering the cross term. With reference to table 1, it can be written as

$$J(k_1^+, k_2^+, X_2 > 0) = \frac{1}{k_1^+ + k_2^+}\left[\frac{P_+(k_1^+)}{k_1^+} - \frac{P_+(k_2^+)}{k_2^+}\right] \times \operatorname{Re}\{A\bar{B}\exp[\mathrm{i}(k_1^+ - k_2^+)X_2] + \bar{A}B\exp[-\mathrm{i}(k_1^+ - k_2^+)X_2]\} \equiv 0,$$

where $A = A_\infty^+(k_1^+)$ and $B = A_\infty^+(k_2^+)$. The cross term vanishes identically and the net downstream flux is made up of direct contributions from the waves $\mathrm{e}^{\mathrm{i}k_1^+ X_2}$ and $\mathrm{e}^{\mathrm{i}k_2^+ X_2}$ only. We write the net flux as

$$J(X_2 > 0) = \frac{|F_0|^2}{4\omega}\left\{|A_\infty^+(k_1^+)|^2\left[\frac{(\omega - Uk_1^+)^2}{k_1^{+2}} + \frac{2U(\omega - Uk_1^+)}{k_1^+} + 4k_1^{+3}\right] + |A_\infty^+(k_2^+)|^2\left[\frac{(\omega - Uk_2^+)^2}{k_2^{+2}} + \frac{2U(\omega - Uk_2^+)}{k_2^+} + 4k_2^{+3}\right]\right\}, \quad \omega_s < \omega < \omega_p, \quad U < U_c. \tag{4.19}$$

By using equation (3.8) and $P_+(k_{1,2}^+) = 0$, we rewrite (4.19) in the form

$$J(X_2 > 0) = \tfrac{1}{4}|F_0|^2 \omega \operatorname{Re}\{k_1^+/P'_+(k_1^+) + k_2^+/P'_+(k_2^+)\}, \quad \omega_s < \omega < \omega_p, \quad U < U_c. \tag{4.20}$$

Equation (4.19) can be rewritten again, in terms of the group velocity and mean energy density. Differentiating $P_+(k, \omega) = 0$ with respect to k we determine the group velocity as

$$\partial\omega/\partial k = 5k^4 - \omega^2 + 2U(\omega - Uk)/2[\omega k + (\omega - Uk)].$$

We may use $P_+(k, \omega) = 0$ to substitute for the square brackets in (4.19), and we then rewrite that equation as

$$J(X_2 > 0) = \tfrac{1}{2}|F_0|^2\left\{|A_\infty^+(k_1^+)|^2\left[1 + \frac{(\omega - Uk_1^+)}{\omega k_1^+}\right]\frac{\partial\omega}{\partial k_1^+} + |A_\infty^+(k_2^+)|^2\left[1 + \frac{(\omega - Uk_2^+)}{\omega k_2^+}\right]\frac{\partial\omega}{\partial k_2^+}\right. \tag{4.21}$$

The downstream flux, given above, is equal to

$$J(X_2 > 0) = T(k_1^+)\frac{\partial\omega}{\partial k_1^+} + T(k_2^+)\frac{\partial\omega}{\partial k_2^+}, \tag{4.22}$$

PHILOSOPHICAL TRANSACTIONS OF THE ROYAL SOCIETY A MATHEMATICAL, PHYSICAL & ENGINEERING SCIENCES

Table 1. *Summary of exact results for the energy fluxes upstream and downstream of the excitation*

(Here $A \equiv F_0 A^+_\infty(k^+_1)$; $B \equiv F_0 A^+_\infty(k^+_2)$; $C \equiv F_0 A^-_\infty(k^-_3)$; $D \equiv F_0 A^-_\infty(k^-_3)$; and $J = J_f + J_{pf} + J_p$. Further each flux is to be multiplied by $1/2\omega$ and the real part taken.)

	downstream		
energy flux term:	k^+_1	k^+_2	cross term
(i) $\omega \leqslant \omega_s$			
J_f	$\dfrac{\lvert A\rvert^2(\omega - Uk^+_1)(\omega - U\overline{k^+_1})\exp[\mathrm{i}k^+_1 - \overline{k^+_1})x]}{k^+_1(k^+_1 + k^+_1)}$	$\dfrac{\lvert B\rvert^2(\omega - Uk^+_2)(\omega - U\overline{k^+_2})\exp[\mathrm{i}(k^+_2 - \overline{k^+_2})x]}{k^+_2(k^+_2 + k^+_2)}$	$\dfrac{A\bar{B}(\omega - Uk^+_1)^2}{k^{+2}_1}$
J_{pf}	$\dfrac{U\lvert A\rvert^2(\omega - Uk^+_1)\exp[\mathrm{i}(k^+_1 - \overline{k^+_1})x]}{k^+_1}$	$\dfrac{U\lvert B\rvert^2(\omega - Uk^+_2)\exp[\mathrm{i}(k^+_2 - \overline{k^+_2})x]}{k^+_2}$	$\dfrac{2UA\bar{B}(\omega - Uk^+_1)}{k^+_1}$
J_p	$\lvert A\rvert^2 k^{+2}_1(k^+_1 + \overline{k^+_1})\exp[\mathrm{i}(k^+_1 - \overline{k^+_1})x]$	$\lvert B\rvert^2 k^{+2}_2(k^+_2 + \overline{k^+_2})\exp[\mathrm{i}(k^+_2 - \overline{k^+_2})x]$	$4A\bar{B}k^{+3}_1$
J	0	0	$\omega^2 k^+_1 / P'_+(k^+_1)$
(ii) $\omega_s \leqslant \omega \leqslant \omega_p$			
J_f	$A^2(\omega - Uk^+_1)^2/2k^{+2}_1$	$B^2(\omega - Uk^+_2)^2/2k^{+2}_2$	$\dfrac{AB(\omega - Uk^+_1)(\omega - Uk^+_2)}{k^+_1 k^+_2}\cos((k^+_1 - k^+_2)x)$
J_{pf}	$UA^2(\omega - Uk^+_1)/k^+_1$	$UB^2(\omega - Uk^+_2)/k^+_2$	$UAB\left[\dfrac{(\omega - Uk^+_2)}{k^+_2} + \dfrac{(\omega - Uk^+_1)}{k^+_1}\right]\cos((k^+_1 - k^+_2)x)$
J_p	$2A^2 k^{+3}_1$	$2B^2 k^{+3}_2$	$AB[k^{+3}_1 + k^{+3}_2 + k^+_1 k^+_2(k^+_1 + k^+_2)]\cos((k^+_1 - k^+_2)x)$
J	$\omega^2 k^+_1 / 2P'_+(k^+_1)$	$\omega^2 k^+_2 / 2P'_+(k^+_2)$	0
(iii) $\omega_p \leqslant \omega$			
J_f	—	$B^2(\omega - Uk^+_2)^2/2k^{+2}_2$	—
J_{pf}	—	$UB^2(\omega - Uk^+_2)/k^+_2$	—
J_p	—	$2B^2 k^{+3}_2$	—
J	—	$\omega^2 k^+_2 / 2P'_+(k^+_2)$	—

PHILOSOPHICAL TRANSACTIONS OF THE ROYAL SOCIETY A MATHEMATICAL, PHYSICAL & ENGINEERING SCIENCES

		upstream	
energy flux term:	k_3^+	k_3^-	cross term
(i) $\omega \leqslant \omega_p$			
J_f	$\frac{1}{2}C^2(\omega-Uk_3^+)^2/k_3^{+2}$	$-\frac{1}{2}D^2(\omega-Uk_3^-)^2/k_3^{-2}$	$-\dfrac{CD(\omega-Uk_3^+)(\omega-Uk_3^-)}{(k_3^+-k_3^-)}\left\{\dfrac{\exp[\mathrm{i}(k_3^+-k_3^-)x]}{k_3^+}+\dfrac{\exp[-\mathrm{i}(k_3^+-k_3^-)x]}{k_3^-}\right\}$
J_{pf}	$UC^2(\omega-Uk_3^+)/k_3^+$	$-UD^2(\omega-Uk_3^-)/k_3^-$	$UCD\left\{\dfrac{(\omega-Uk_3^+)\exp[\mathrm{i}(k_3^+-k_3^-)x]}{k_3^+}-\dfrac{(\omega-Uk_3^-)\exp[-\mathrm{i}(k_3^+-k_3^-)x]}{k_3^-}\right\}$
J_p	$2C^2k_3^{+3}$	$2D^2k_3^{-3}$	$CD(k_3^++k_3^-)\{k_3^{+2}\exp[\mathrm{i}(k_3^+-k_3^-)x]+k_3^{-2}\exp[-\mathrm{i}(k_3^+-k_3^-)x]\}$
J	$\omega^2k_3^+/2P'_+(k_3^+)$	$\omega^2k_3^-/2P'_-(k_3^-)$	0
(ii) $\omega_p \leqslant \omega$			
J_f	—	$-\frac{1}{2}D^2(\omega-Uk_3^-)^2/k_3^{-2}$	—
J_{pf}	—	$-UD^2(\omega-Uk_3^-)/k_3^-$	—
J_p	—	$2D^2k_3^{-3}$	—
J	—	$\omega^2k_3^-/2P'_-(k_3^-)$	—

where

$$T(k_n^+) = (|F_0|^2/4\omega^2)|A_\infty^+(k_n^+)|^2[\omega^2 + k_n^{+4} + (\omega - Uk_n^+)^2/k_n^+ + 2U(\omega - Uk_n^+)] \quad (4.23)$$

represents the mean energy density associated with the particular wave $e^{ik_n^+ x}$. The expressions for $T(k_1^+), T(k_2^+)$ are found by calculating the total time averaged mean energy density per unit length of Ox. (Details are given for the single downstream wave case in the next paragraph.)

For frequencies in the range $\omega_p < \omega$, the root k_1^+ has a positive imaginary component and the wave generated decays exponentially as it propagates downstream. The root k_2^+ is real and is given to second order (for $U^{\frac{5}{3}} \ll \omega \ll U^{\frac{5}{4}}$) by

$$k_2^+ = \omega^{\frac{2}{5}} - 2U/5\omega^{\frac{1}{5}},$$

though again the following results are *exact*. The wave generated is outgoing and stable and it alone is used to calculate the energy terms. The net flux is found to be

$$J(X_2 > 0) = \frac{|F_0|^2 |A_\infty^+(k_2^+)|^2}{4\omega}\left[\frac{(\omega - Uk_2^+)^2}{k_2^{+2}} + \frac{2U(\omega - Uk_2^+)}{k_2^+} + 4k_2^{+3}\right] = \tfrac{1}{4}|F_0|^2\omega \,\mathrm{Re}\{k_2^+/P'_+(k_2^+)\} \quad (4.24)$$

$$= \tfrac{1}{2}|F_0|^2 |A_\infty^+(k_2^+)|^2\left[1 + \frac{(\omega - Uk_2^+)}{\omega k_2^+}\right]\frac{\partial\omega}{\partial k_2^+}, \quad \text{when } \omega_p < \omega, \text{ with } U < U_c. \quad (4.25)$$

We can write the flux in terms of the mean energy density and the group velocity. To check this result we calculate the time averaged wave energy density per unit length of Ox. The time averaged kinetic energy in the plate, per unit length, is

$$T_p = \tfrac{1}{4}\,\mathrm{Re}\{\eta_t \overline{\eta_t}\} = \tfrac{1}{4}|F_0|^2 |A_\infty^+(k_2^+)|^2,$$

and the associated mean elastic energy in the plate is

$$V_p = \tfrac{1}{4}\,\mathrm{Re}\{\eta_{xx}\overline{\eta_{xx}}\} = \tfrac{1}{4}|F_0|^2 |A_\infty^+(k_2^+)|^2 k_2^{+4}/\omega^2.$$

The corresponding fluid energy T_f is made up of two contributions, as in (4.4),

$$T_f = \frac{|F_0|^2 |A_\infty^+(k_2^+)|^2}{4\omega^2}\frac{(\omega - Uk_2^+)^2}{k_2^+} + \frac{U(\omega - Uk_2^+)}{2\omega k_2^+}\,\mathrm{Re}\{-iF_0 A_\infty^+(k_2^+)\, e^{ik_2^+ x} e^{-k_2^+ \bar{\eta}}\}.$$

The total mean energy density T is the sum of T_p, V_p and T_f, and after substitution using $P_+(k_2^+) = 0$, we find that

$$T(k_2^+) = \tfrac{1}{2}|F_0|^2 |A_\infty^+(k_2^+)|^2[1 + (\omega - Uk_2^+)/\omega k_2^+]. \quad (4.26)$$

Equation (4.25) then gives us the required result, namely

$$J(X_2 > 0) = T(k_2^+)\,\partial\omega/\partial k_2^+, \quad \text{when} \quad \omega_p < \omega, \quad \text{with} \quad U < U_c. \quad (4.27)$$

Thus the flux is associated with propagation of the energy density at the group velocity when the single neutral wave propagates downstream ($\omega > \omega_p$); and (4.22) states that in the range $\omega_s < \omega < \omega_p$, when two neutral waves propagate downstream, the flux is composed simply of the sum of the two energy-density–group-velocity products. On the other hand, in the unstable range $0 < \omega < \omega_s$, the flux arises solely from *interaction* between the decaying and amplifying waves.

The roots $k_3^\pm$ generate waves upstream of the drive point. For all $\omega \ll \omega_p$ the roots are given, to second order, by

$$k_3^\pm = \pm U^{\frac{2}{3}} - 2\omega/3U.$$

The roots are real and one incoming wave ($e^{ik_3^+ x}$) and one outgoing wave ($e^{ik_3^- x}$) are seen in the upstream far field. The energy flux terms are evaluated exactly using both waves, and cross terms occur. The results are summarized in table 1. We consider the cross term first. With $k_3^\pm$ real, we find that $P'_+(k_3^+)$, $P'_-(k_3^-)$ and $A_\infty^-(k_3^\pm)$ are real. The cross term can be rearranged to yield

$$J(k_3^+, k_3^-, X_1 < 0) = |F_0|^2(\omega^2 - k_3^{+2}k_3^{-2})/2\omega(k_3^+ - k_3^-)$$
$$\times A_\infty^-(k_3^+) A_\infty^-(k_3^-) \operatorname{Re}\{\exp[i(k_3^+ - k_3^-)X_1] - \exp[-i(k_3^+ - k_3^-)X_1]\} \equiv 0.$$

Hence the net flux in the downstream direction (at a point upstream of the drive) is given by

$$J(X_1 < 0) = \frac{|F_0|^2}{4\omega}\left\{|A_\infty^-(k_3^+)|^2\left[\frac{(\omega - Uk_3^+)^2}{k_3^{+2}} + \frac{2U(\omega - Uk_3^+)}{k_3^+} + 4k_3^{+3}\right]\right.$$
$$\left. + |A_\infty^-(k_3^-)|^2\left[-\frac{(\omega - Uk_3^-)^2}{(k_3^-)^2} - \frac{2U(\omega - Uk_3^-)}{k_3^-} + 4(k_3^-)^3\right]\right\} \tag{4.28}$$

$$= \tfrac{1}{4}|F_0|^2\omega \operatorname{Re}\left\{\frac{k_3^+}{P'_+(k_3^+)} + \frac{k_3^-}{P'_-(k_3^-)}\right\}. \tag{4.29}$$

Equation (4.28) can be rewritten in terms of group velocity and mean energy density as

$$J(X_1 < 0) = \tfrac{1}{2}|F_0|^2\left\{|A_\infty^-(k_3^+)|^2\left[1 + \frac{(\omega - Uk_3^+)}{k_3^+}\right]\frac{\partial\omega}{\partial k_3^+} + |A_\infty^-(k_3^-)|^2\left[1 - \frac{(\omega - Uk_3^-)}{k_3^-}\right]\frac{\partial\omega}{\partial k_3^-}\right\}, \tag{4.30}$$

and this is of the same form as (4.22).

With the frequency in the range $\omega_p < \omega$, the root k_3^+ has a negative imaginary component and the wave generated decays. The root k_3^- is given to second order (for $U^{\frac{5}{3}} \ll \omega \ll U^{\frac{5}{4}}$) by

$$k_3^- = -\omega^{\frac{2}{5}} - 2U/5\omega^{\frac{1}{5}},$$

and it generates a stable outgoing wave. The results are summarized in table 1, and are precisely those given above in equations (4.28) and (4.29) for the wave $e^{ik_3^- x}$ alone, together with the relevant expression for k_3^-.

4.4. *Confirmation of equation* (4.11)

Using the results of the previous section, and with (4.11) in mind, we determine the net flux difference between station $X_2 > 0$ (downstream) and $X_1 < 0$ (upstream) as follows.

(i) $\omega < \omega_s$, $J(X_2) - J(X_1) = \tfrac{1}{4}|F_0|^2\omega \operatorname{Re}\left\{\frac{k_1^+}{P'_+(k_1^+)} + \frac{k_2^+}{P'_+(k_2^+)} - \frac{k_3^+}{P'_+(k_3^+)} - \frac{k_3^-}{P'_-(k_3^-)}\right\}$,

(ii) $\omega_s < \omega < \omega_p$, $J(X_2) - J(X_1) = \tfrac{1}{4}|F_0|^2\omega \operatorname{Re}\left\{\frac{k_1^+}{P'_+(k_1^+)} + \frac{k_2^+}{P'_+(k_2^+)} - \frac{k_3^+}{P'_+(k_3^+)} - \frac{k_3^-}{P'_-(k_3^-)}\right\}$,

(iii) $\omega_p < \omega$, $J(X_2) - J(X_1) = \tfrac{1}{4}|F_0|^2\omega \operatorname{Re}\left\{\frac{k_2^+}{P'_+(k_2^+)} - \frac{k_3^-}{P'_-(k_3^-)}\right\}$.

For the remaining term in (4.11), we have

$$I_0 = \tfrac{1}{2}|F_0|^2 \operatorname{Re} A_0^* = |F_0|^2 \omega \operatorname{Re}\{\mathrm{i}\Psi(0)\}/4\pi. \tag{4.31}$$

We determine $\Psi(0)$ in the Appendix. Using the results we rewrite I_0 as

$$I_0 = \tfrac{1}{4}|F_0|^2 \omega \operatorname{Re}\left\{\frac{k_1^+}{P'_+(k_1^+)} + \frac{k_2^+}{P'_+(k_2^+)} - \frac{k_3^+}{P'_+(k_3^+)} - \frac{k_3^-}{P'_-(k_3^-)}\right\}. \tag{4.32}$$

For frequency in the range $\omega < \omega_s$, the system is convectively unstable. I_0 is given by (4.32), and comparing this with (i) above we see that

$$I_0 \equiv J(X_2) - J(X_1), \quad \text{for} \quad \omega < \omega_s, \tag{4.33}$$

and equation (4.11) is satisfied. With frequency in the range $\omega_s < \omega < \omega_p$, I_0 is again given by (4.32). On comparison with (ii) above we again find that equation (4.11) is satisfied for $\omega_s < \omega < \omega_p$.

With frequency in the range $\omega_p < \omega$, we have the fact that $k_1^+ = k_3^+$, and hence

$$\operatorname{Re}\{k_1^+/P'_+(k_1^+) - k_3^+/P'_+(k_3^+)\} = 0.$$

Equation (4.32) is thereby reduced, and on comparison with (iii) above we again check that equation (4.11) is satisfied in this high-frequency range.

4.5. *Evaluation and properties of* $\operatorname{Re} A_0$

Equations (4.31) and (4.32) give an explicit expression for the real part of the drive point admittance,

$$\operatorname{Re} A_0 = \tfrac{1}{2}\omega \operatorname{Re}\left\{\frac{k_1^+}{P'_+(k_1^+)} + \frac{k_2^+}{P'_+(k_2^+)} - \frac{k_3^+}{P'_+(k_3^+)} - \frac{k_3^-}{P'_-(k_3^-)}\right\}. \tag{4.34}$$

Using equations (2.15), (2.16) and (2.25) we can substitute into (4.34) to determine $\operatorname{Re} A_0$ approximately when $\omega = \Omega U^2, \Omega = O(1)$. We find

$$\operatorname{Re} A_0 \sim -(\omega/2U^2)\{1 + \tfrac{16}{9}(\Omega U)^{\frac{1}{3}} + \tfrac{100}{3}\Omega^3 U\}. \tag{4.35}$$

Using the results of §3 we find also that for $\omega_p < \omega$, $O(U^{\frac{5}{3}}) < \omega < O(1)$, $\operatorname{Re} A_0 = 1/5\omega^{\frac{1}{5}}$ (by equation (3.11)), and for $\omega_p < \omega$, $O(1) < \omega$, $\operatorname{Re} A_0 = 1/4\omega^{\frac{1}{2}}$ (by equation (3.12)). These approximations to $\operatorname{Re} A_0$ are plotted against the exact numerically calculated values of $\operatorname{Re} A_0$ in figures 4 and 5 for the appropriate frequency ranges and for $U = 0.05$.

To determine $\operatorname{Re} A_0$ around $\omega = \omega_p$ we concentrate on

$$\Delta = \frac{k_1^+}{P'_+(k_1^+)} - \frac{k_3^+}{P'_+(k_3^+)}.$$

Referring to Brazier-Smith & Scott (1984, equation (3.3)), we write the two complex conjugate poles k_1^+, k_3^+ (for $\omega > \omega_p$) as

$$k_{1,3}^+ \approx k_p \pm \mathrm{i}\lambda(\omega - \omega_p)^{\frac{1}{2}}, \tag{4.36}$$

where $\lambda = (2(\partial D/\partial\omega)/(\partial^2 D/\partial k^2))^{\frac{1}{2}}$. We determine $P'_+(k_{1,3}^+)$, using a Taylor expansion about k_p, as

$$P'_+(k_{1,3}^+) = A(k_p, \omega) \pm \mathrm{i}B(k_p, \omega),$$

where $$A(k_p, \omega) = -(\lambda^2/2!)(\omega - \omega_p) P_+^{(\mathrm{iii})}(k_p) + (\lambda^4/4!)(\omega - \omega_p)^2 P_+^{(\mathrm{v})}(k_p)$$

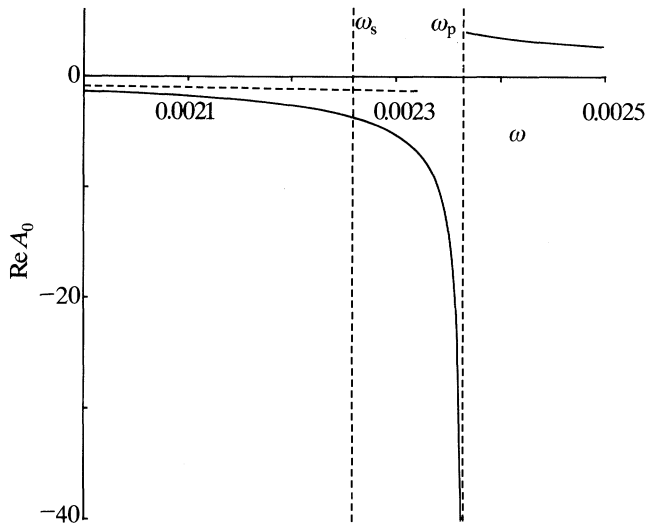

Figure 4. Plot of $\mathrm{Re}\,A_0$, and comparison with the low-frequency approximation (4.35), (– – –) for $U = 0.05$ and $0.002 \leqslant \omega \leqslant 0.0025$.

and $$B(k_p, \omega) = \lambda(\omega-\omega_p)^{\frac{1}{2}}P_+^{(ii)}(k_p) - (\lambda^3/3!)(\omega-\omega_p)^{\frac{3}{2}}P_+^{(iv)}(k_p).$$

Upon evaluation we find, as expected, that $\mathrm{Re}\,\Delta \equiv 0$ for all $\omega > \omega_p$, and

$$\mathrm{Re}\,A_0 = \mathrm{Re}\left\{\frac{k_2^+}{P'_+(k_2^+)} - \frac{k_3^-}{P'_-(k_3^-)}\right\} = O(1) \quad \text{as} \quad \omega \to \omega_p + 0.$$

With $\omega < \omega_p$, $(\omega-\omega_p)^{\frac{1}{2}} = e^{\pi i/2}|\omega-\omega_p|^{\frac{1}{2}}$. Substitution into the expressions for $k_{1,3}^+$ yields

$$k_{1,3}^+ = k_p \mp \lambda|\omega-\omega_p|^{\frac{1}{2}}.$$

We determine $P'_+(k_{1,3}^+)$ as

$$P'_+(k_{1,3}^+) \simeq \mp\lambda|\omega-\omega_p|^{\frac{1}{2}}P''_+(k_p)\left[1 \mp \frac{\lambda|\omega-\omega_p|^{\frac{1}{2}}}{2!}\frac{P'''_+(k_p)}{P''_+(k_p)}\right],$$

and Δ as $$\Delta \approx -2k_p/\lambda|\omega-\omega_p|^{\frac{1}{2}}P''_+(k_p), \tag{4.37}$$

which clearly is singular as $\omega \to \omega_p - 0$.

Equation (4.34) can of course be evaluated numerically. Figure 4 is a plot of $\mathrm{Re}\,A_0$ for $U = 0.05$, and frequency in the range $0.002 \leqslant \omega \leqslant 0.0025$. We see that $\mathrm{Re}\,A_0$ is negative for $\omega < \omega_p = 0.0023649$ and positive for all $\omega > \omega_p$. As predicted by the analysis $\mathrm{Re}\,A_0$ tends to negative infinity as $\omega \to \omega_p, \omega < \omega_p$, and is well behaved for $\omega > \omega_p$. $\mathrm{Re}\,A_0$ passes smoothly through the double root at $\omega = \omega_s = 0.0022589$. The low-frequency approximation (4.35) to $\mathrm{Re}\,A_0$ is also plotted on figure 4, indicated by the dashed line.

In figure 5 we plot the exact $\mathrm{Re}\,A_0$ of (4.34) against the high-frequency approximation of (3.12) and the moderate frequency approximation of (3.11), with $U = 0.05$. Plot (*a*) demonstrates that there is a frequency band well within the limits $O(U^{\frac{5}{3}}) < \omega < O(1)$ in which the $\mathrm{Re}\,A_0$ of (4.34) and that of (3.11) agree. Plot (*b*) demonstrates close agreement between $\mathrm{Re}\,A_0$ and the real part of (3.12) for $\omega > 10$.

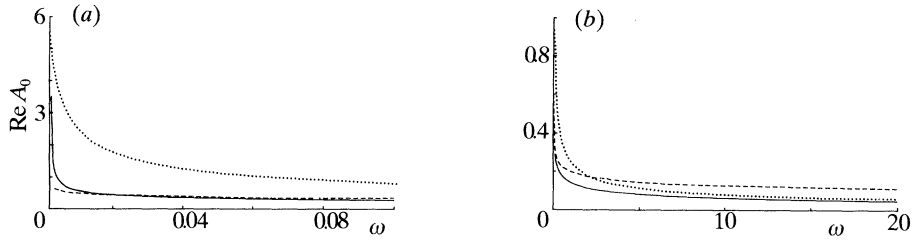

Figure 5. Plot of $\mathrm{Re}\, A_0$ against high frequency (....) approximation (3.12) and moderate frequency (– – –) approximation (3.11), with $U = 0.05$ and (*a*) $0.002 < \omega < 0.1$, (*b*) $0.002 < \omega < 20$.

The significant conclusion is that the negative values of $\mathrm{Re}\, A_0$ persist throughout the range $0 < \omega < \omega_p$, thus including the range $\omega_s < \omega < \omega_p$ in which there are no convective instabilities as well as the range $0 < \omega < \omega_s$ of convective instability. Only in the range $\omega > \omega_p$ is the energy input *from* the driver into the fluid–plate system. Note also that quite different results would be produced by the use of the conventional integration contour (indented above singularities on the negative real axis and below any on the positive) rather than the deformed *causal* contour which is necessary in general; even in the stable range $\omega_s < \omega < \omega_p$. This range, $\omega_s < \omega < \omega_p$ may well be called one of anomalous neutral stability, a title further justified by the results to be given in §5.

5. Negative energy wave aspects

5.1. *Introduction to negative energy*

Although many of the results given earlier have been exact, they are perhaps most easily understood for frequencies in the convectively unstable régime $\omega < \omega_s(U)$. The frequency range $\omega_s(U) < \omega < \omega_p(U)$ is one in which all the wavenumbers $k_1^+, k_2^+, k_3^\pm$ are real, but in which there are highly unusual features which warrant the name 'anomalous neutral propagation' range for such frequencies. Some clarification of the situation in this range can be obtained from the ideas of the theory of positive and negative energy waves, to which we now turn.

A problem that involves a flexible solid coupled to a flow can be described as a 'flutter problem' or as a 'compliant surface problem', and instabilities are always to be expected. Benjamin (1960) determined that three distinct types of instability were possible and they were later classified by Landahl (1962) and Benjamin (1963) as 'class A', 'class B' and 'class C', or 'Kelvin–Helmholtz', instabilities.

Class A and class B instabilities are essentially degenerate stable waves. They consist of energy conserving oscillations which become unstable when subjected to an irreversible process. To classify the instabilities Landahl (1962) and Benjamin (1963) looked at the 'activation energy' (Benjamin's terminology) of the waves. The activation energy ($\bar{E}$) is the net energy required from an external agency to create a given steady state wave from rest in a non-conservative system. Benjamin and Landahl recognized that the generation of a class A oscillation leads to an overall decrease in the energy of the system. This type of wave has negative activation energy and is henceforth known as a NEW ($\bar{E} < 0$). NEWs are destabilized by damping, which leads to their growth, because the energy level of the wave decreases below the activation level and the value of $|E|$ is increased (where E is the total energy of the wave). Since $|E|$ is proportional to (amplitude)^2, this is the mechanism by which loss of energy by a NEW results in an increase in its wave amplitude.

The generation of a class B oscillation leads to an overall increase in the energy of the system, and class B oscillations are known as PEWS ($\bar{E} > 0$). Damping of a PEW leads to energy decrease below the activation level (now positive), and thus to decay.

Class C instabilities have no stable counterpart. They exist when there is a unidirectional transfer of energy from the flow into the solid; there is therefore no net change in the energy level of the system and the activation energy level is zero.

Benjamin calculated the activation energy $\bar{E}$, in the non-conservative system, by subtracting the energy W lost by the fluid, per unit area of the boundary, from the sum of the mean kinetic and potential energies per unit area of the interface, T and V respectively. Cairns (1979) derived an expression for the total energy of the wave as

$$E = \tfrac{1}{4}(\omega\,\partial D_1/\partial\omega)|A|^2, \tag{5.1}$$

where ω and A are the frequency and amplitude of the surface wave deflexion, and $D_1(k,\omega)$ is a dispersion function defined in a certain precise way by Cairns; when applied to the present problem, Cairns' method leads to the identification of $D_1(k,\omega)$ given in (5.5) below. Expression (5.1) is derived by calculating the work done during an idealized process in which a wave is generated by an external driving force applied to the surface of the fluid. Use of equation (5.1) makes for easy identification of PEW ($E > 0$) and NEW ($E < 0$).

In §4, equation (4.23), we calculated the total mean energy density $T(k_n)$ of a stable wave of wavenumber k_n. We now find that T is equivalent to Benjamin's $\bar{E}$, except that where he subtracts the energy lost by the fluid we add on the energy gained by it. We also find that our T is equal to the E of Cairns, provided we take $D_1 = -D$ where $D(k,\omega)$ is the dispersion function of §2.

5.2. *Neutral waves on the fluid-loaded plate with mean flow*

The problem we now solve is as stated in §2.1 with one change; the fixed-frequency time-harmonic forcing $F(t) = F_0 \exp(-\mathrm{i}\omega_0 t)$ is absent, and we look at the free propagation of a wave of fixed real wavenumber k, concentrating on the case when the frequency ω is also real. Thus we consider a surface displacement

$$\eta(x,t) = A\exp(\mathrm{i}kx - \mathrm{i}\omega t) \tag{5.2}$$

with k real. In §2 we found expressions for the roots of $P_{\pm}(k) = 0$. In particular we determined for which frequencies the roots were real and would generate waves of the type which we now take as the surface displacement. Equation (5.2) corresponds to the response downstream of the drive point for $\omega_s < \omega < \omega_p$ when there exist two neutrally stable right-running travelling waves, with wavenumbers given approximately by (2.15),

$$k \approx \omega/U \pm (\omega/U)^{\frac{3}{2}}(\omega^2/U^4 - 1)^{\frac{1}{2}},$$

which we consider independently. A right-running stable travelling wave is also seen downstream of the drive point if $\omega > \omega_p$; and upstream of the drive point both a left-running (upstream) and a right-running (downstream) stable travelling wave are seen for all $\omega < \omega_p$, and just the first of these two for $\omega > \omega_p$.

The results for the pressure and velocity potential are

$$p(x,t) = -A((\omega - Uk)^2/\gamma(k))\,\mathrm{e}^{\mathrm{i}kx}\,\mathrm{e}^{-\gamma(k)y}\,\mathrm{e}^{-\mathrm{i}\omega t}, \tag{5.3}$$

$$\phi(x,t) = \mathrm{i}A((\omega - Uk)/\gamma(k))\,\mathrm{e}^{\mathrm{i}kx}\,\mathrm{e}^{-\gamma(k)y}\,\mathrm{e}^{-\mathrm{i}\omega t}, \tag{5.4}$$

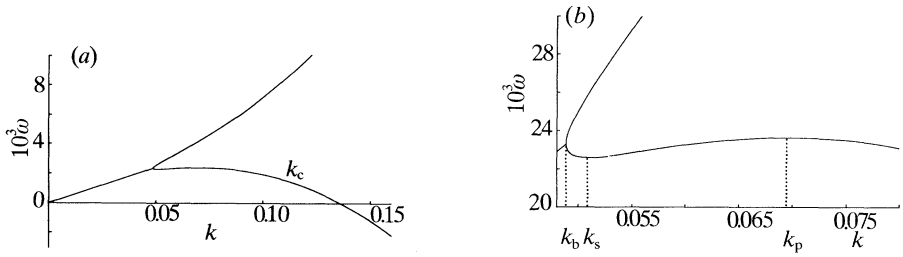

Figure 6. The dispersion curve for neutral waves in the system, with the plate at rest.

where again, for incompressible fluid, the function $\gamma(k) = |k|$ for real k. Equating the pressure difference across the plate to the mass-acceleration product minus the elastic restoring force, we determine the dispersion function in the Cairns (1979) sense as

$$D_1(k,\omega) = \omega^2 - k^4 + (\omega - Uk)^2/\gamma(k), \tag{5.5}$$

Solving $D_1(k,\omega) = 0$ for ω yields two roots,

$$\omega = (k/(1+k))\,[U \pm [k(k^3+k^2-U^2)]^{\frac{1}{2}}]. \tag{5.6}$$

The dispersion curve is shown in figure 6. For real negative k the dispersion curve is given by point reflexion in the origin, since evidently $\omega(-k) = -\omega(k)$. There is a branch point at (k_b, ω_b), where k_b is the (unique) positive root of

$$k^3 + k^2 - U^2 = 0, \tag{5.7}$$

namely
$$k_b = -\tfrac{1}{3} - \tfrac{2}{3}\cos(\tfrac{1}{3}\phi + \tfrac{2}{3}\pi), \tag{5.8}$$

where
$$\phi = \arccos(1 - \tfrac{27}{2}U^2), \quad 0 \leqslant \phi < \tfrac{1}{2}\pi,$$

and the corresponding value of ω is

$$\omega_b = Uk_b/(1+k_b). \tag{5.9}$$

For $|k| < k_b$, equation (5.6) produces complex ω; if $\operatorname{Im}\omega < 0$ the wave decays, but if $\operatorname{Im}\omega > 0$, the wave grows exponentially with time. Thus, for any $|k| < k_b$, a temporal instability is generated and this corresponds to the class C or Kelvin–Helmholtz instability of Benjamin.

For $|k| > k_b$, ω is real and the system is stable. For $k^3 < U^2 < k^3 + k^2$ the dispersion curve has two branches in the first quadrant. At $k = k_c \equiv U^{\frac{2}{3}}$ the lower branch crosses the k-axis into the fourth quadrant.

We note that for small $\omega\,(>0$ say), there are evidently two real roots for k, and these are close to the crossing points, $k \sim \pm|k_c| = \pm U^{\frac{2}{3}}$. These are, of course, the wavenumbers identified earlier as $k_3^{\pm}$, one left-propagating ($k_3^- \sim -U^{\frac{2}{3}}$), one right-propagating ($k_3^+ \sim +U^{\frac{2}{3}}$). However, our earlier analysis from the causality viewpoint showed that these waves are both to be found upstream of any point of localized excitation, a feature not evident from inspection of the dispersion pattern of figure 6 alone.

The group velocity of the waves is given by

$$v_g = \frac{\partial\omega}{\partial k} = \frac{1}{(1+k)^2}\left[U \pm \frac{k[3k^4+5k^3+2k^2+(3+k)(k^3+k^2-U^2)]}{2[k(k^3+k^2-U^2)]^{\frac{1}{2}}}\right]. \tag{5.10}$$

At the branch point the group velocity becomes infinite. The lower branch has turning points when the group velocity is zero. At these points, ω locally has quadratic variation with k, and therefore the frequencies concerned are real branch points for k as a function of ω. They must therefore correspond to the two real frequencies $\omega_s(U)$ and $\omega_p(U)$ identified earlier. Only one of these, ω_p, corresponds to a 'pinch', and terminates the frequency range of anomalous neutral propagation; the other corresponds to a merging of amplifying and decaying instability waves, terminating the convectively unstable frequency range.

Squaring and solving for U^2 we determine expressions for U^2, at the turning points, as

$$U^2 = \frac{2k^2}{4+9k+6k^2+k^3}\{(1+\tfrac{17}{2}k+16k^2+\tfrac{21}{2}k^3+2k^4) \pm (1-8k-42k^2-68k^3-47k^4-12k^5)^{\frac{1}{2}}\},$$

and for $U \ll 1$ we determine the turning points to lowest order as

$$k_s \sim U, \quad k_p \sim (\tfrac{4}{25})^{\frac{1}{3}}U^{\frac{2}{3}}, \tag{5.11}$$

with k_s, k_p corresponding to ω_s, ω_p respectively. These correspond to $\omega_s \sim U^2, \omega_p \sim NU^{\frac{5}{3}}$ as given in (2.17) and (2.21) respectively, and higher approximations can be found corresponding to those in (2.18) and (2.22). For $U = 0.05$ we read off from figure 6 values of ω_s, ω_p which are exactly those computed for this case by Brazier-Smith & Scott (1984).

For the branch point (ω_b, k_b) we find from (5.7) and (5.8) that

$$\begin{aligned} k_b &= U-\tfrac{1}{2}U^2+O(U^3), \\ \omega_b &= U^2(1-\tfrac{3}{2}U+O(U^3)), \end{aligned} \tag{5.12}$$

which shows that $\omega_s < \omega_b < \omega_p$. The second of (5.12) gives $\omega_b = 0.0023125$ for $U = 0.05$, and the exact value is 0.0023277.

We note that for $k_b < k < k_s$ and $k > k_p$ the lower branch of figure 6 has negative group velocity v_g, and positive group velocity for $k_s < k < k_p$. On the upper branch the group velocity is positive throughout. For the wave energy we use Cairns' expression (5.1) and evaluate $\partial D_1/\partial\omega$ on the dispersion curve to get

$$\partial D_1/\partial\omega = \pm 2[k(k^3+k^2-U^2)]^{\frac{1}{2}}, \tag{5.13}$$

positive on the upper branch, negative on the lower. Therefore the upper branch has $\omega > 0, \partial D_1/\partial\omega > 0, v_g > 0$ and is a PEW with energy flux

$$J = v_g E, \tag{5.14}$$

directed in the positive x-direction (as also is the phase velocity). We might expect to see such a wave downstream of a point of local excitation. This is indeed the case, and the wave concerned was indicated by wavenumber k_2^+ in §§2–4. However, such a wave was then found downstream throughout $\omega > \omega_s$, whereas we find it now only for $\omega > \omega_b$. The reason is that the lower branch of the dispersion curve also corresponds to k_2^+ for $k_b < k < k_s$, in which range we have $\omega > 0, E < 0, v_g < 0$. Thus the k_2^+ wave is actually a NEW in this range with negative (leftward) group velocity, but the energy flux is positive and the wave continues to appear downstream of a point of local excitation.

As just observed, the lower branch has $\omega > 0$ and $\partial D_1/\partial\omega < 0$ throughout $k_b <$

Table 2. *Summary of properties of neutrally stable waves corresponding to the two branches of the dispersion curve for different wavenumber ranges*

(In the last column U and D indicate that the wave is found upstream or downstream of a point of excitation respectively.)

	ω	$\partial D_1/\partial\omega$	E	v_g	J	k	location
upper branch							
$k > k_b$	+	+	+	+	+	k_2^+	D
lower branch							
$k_b < k < k_s$	+	−	−	−	+	k_2^+	D
$k_s < k < k_p$	+	−	−	+	−	k_1^+	D
$k_p < k < k_c$	+	−	−	−	+	k_3^+	U
$k_c < k$	−	−	+	−	−	k_3^-	U

$k < k_c$, and so represents a NEW. It has $v_g < 0$ for $k_b < k < k_s$ and $k_p < k < k_c$, $v_g > 0$ for $k_s < k < k_p$. The range $k_b < k < k_s$ corresponds to the wave with wavenumber k_2^+, as just discussed, while for $\omega_s < \omega < \omega_p$ and $k_s < k < k_p$ the lower branch wavenumber must be that denoted by k_1^+ earlier. This (k_1^+) wave is a NEW with $v_g > 0$ and energy flux $J < 0$, but despite this last feature it appears downstream of a drive point, where its negative energy flux contributes to the energy absorption there ($\mathrm{Re}\, A_0 < 0$ for all $\omega < \omega_p$).

The final right-hand part of the dispersion curve has been mentioned before; it corresponds to wavenumber k_3^+ for $0 < \omega < \omega_p$, a NEW with $v_g < 0, J > 0$. It is found upstream of a drive point, and its positive flux (inward, towards the drive point) also contributes to the energy absorption at the drive point.

For $k > k_c$ the lower branch has $\omega < 0$ and $\partial D_1/\partial\omega < 0$, so that $E > 0$ and the wave is a PEW. The change in sign of E is associated with that of ω alone, and although v_g remains negative the phase velocity changes sign at $k = k_c$. This wave was given wavenumber $(-k_3^-)$ in earlier sections because ω was then always taken positive. The wave appears upstream of the drive point, has v_g and J both negative, and carries energy away from the drive point. It has no unusual features, and for sufficiently high k (or ω) it takes on the character of the familiar leftward propagating bending wave on the plate. The rightward propagating bending wave corresponds to the high-frequency limit along the upper branch. These results are summarized on table 2.

It will be noted that this re-interpretation of the dispersion function from the viewpoint of figure 6 is entirely consistent with earlier results. Thus, for example, k_1^+ and k_3^+ coincide at ω_p, while k_1^+ and k_2^+ coincide at ω_s. However, examination of the situation for complex ω and k is needed to show, as in §3, that k_1^+ and k_3^+ pinch at ω_p, whereas k_1^+ and k_2^+ coincide but do not pinch at ω_s. Clearly there are highly anomalous features of the range $\omega_s < \omega < \omega_p$, although these have been to some extent clarified by recognition of the importance of the sign of E as well as that of v_g. However, Brazier-Smith & Scott's discussion of the wave (k_2^+) in this frequency range is in error. That wave does not have $J < 0$, and in fact has v_g and E both negative for $\omega_s < \omega < \omega_b$ and both positive for $\omega > \omega_b$, and thus downstream-directed energy flux in both cases.

This brings us to the most strikingly anomalous feature; in the range $\omega_s < \omega < \omega_b$, the k_2^+ wave has $v_g < 0$ but it is found downstream of the drive point. This is because wavenumber $k_2^+(\omega)$ starts at infinity in $\mathrm{Im}\, k > 0$ for $\mathrm{Im}\, \omega = +\infty$, and so the k-contour must always pass beneath $k = k_2^+$. However the global behaviour is not

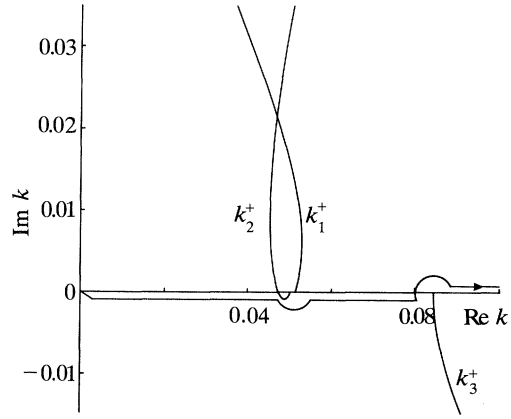

Figure 7. Plot of k_1^+, k_2^+ and k_3^+ in the anomalous frequency range, as $\mathrm{Im}\,\omega$ increases from zero to large positive values.

mimicked by the local behaviour for small positive $\mathrm{Im}\,\omega$. That local behaviour consists of displacement of $k_2^+(\omega)$ first into $\mathrm{Im}\,k < 0$ and only for larger values of $\mathrm{Im}\,\omega > 0$ of ultimate recession to $\mathrm{Im}\,k = +\infty$ (see figure 7 for a particular case). Use of the local behaviour to remove real axis pole singularities, and thereby to pick up wave motions in regions of space only where the waves have group velocity directed away from a region of excitation, is the basis of the method introduced by Lighthill (1960, 1978) for correct selection of 'radiating' waves. However, as discussed in §1, Lighthill made the case for his criterion very clear; the excitation must be the *source* of all the wave energy, and in our problem it is not. Indeed the role of the excitation is one of wavenumber and energy *conversion*, the inhomogeneity on the plate acting as a mechanism for transferring energy from the large reservoir in the free stream to wave energy.

There is therefore no conflict with the Lighthill criterion, and no need to argue that the anomalous neutral waves would never be seen in practice because they would be exponentially small compared with the convectively unstable waves with frequencies in $0 < \omega < \omega_s$ that would necessarily be generated in any start-up process. The propagating waves, whether amplifying or not, correspond to residue contributions which quickly dominate the branch line integral, and then because the amplifying waves have only a small growth rate (see (2.23)) it is quite possible that they will not dominate the anomalous neutral waves until x has attained very large values indeed.

5.3. *Comments on the energy fluxes*

Using table 1 and the approximate expressions for the roots, it is possible to calculate the order of magnitude and the direction of the fluxes. The results are summarized on table 3. We begin with the downstream results. We have demonstrated that for any frequency less than ω_s, the total flux J across any station due directly to the exponentially growing or decaying wave is zero. However, the individual fluxes $J_f(k_1^+)$, $J_{pf}(k_1^+)$, etc., are not zero. Ignoring exponentially large and small terms, it is clear that the significant fluxes are the fluid and plate–fluid fluxes. These fluxes have opposite directions, with the energy associated with the fluid–plate flux always travelling upstream towards the drive point. The energy in the fluid and in the plate is always right running.

Table 3. *Summary of approximate results for the energy fluxes upstream and downstream of the excitation*

(Each flux is to be multiplied by $|F_0|^2$, and only the leading order term is quoted in each entry.)

	downstream		
energy flux term:	k_1^+	k_2^+	cross term
(i) $\omega \ll \omega_s$			
J_f	$\frac{1}{16}(\omega/U^2)\exp(-2(\omega/U)^{\frac{3}{2}}x)$	$\frac{1}{16}(\omega/U^2)\exp(2(\omega/U)^{\frac{3}{2}}x)$	$\frac{1}{8}(\omega/U^2)$
J_{pf}	$-\frac{1}{16}(\omega/U^2)\exp(-2(\omega/U)^{\frac{3}{2}}x)$	$-\frac{1}{16}(\omega/U^2)\exp(2(\omega/U)^{\frac{3}{2}}x)$	$-\frac{1}{2}(\omega/U^2)$
J_p	$\frac{1}{4}(\omega^3/U^6)\exp(-2(\omega/U)^{\frac{3}{2}}x)$	$\frac{1}{4}(\omega^3/U^6)\exp(2(\omega/U)^{\frac{3}{2}}x)$	$-\frac{1}{2}(\omega^3/U^6)$
J	0	0	$-\frac{3}{8}(\omega/U^2)$
(ii) $\omega_s \ll \omega \ll \omega_p$			
J_f	$\frac{1}{16}(\omega/U^2)$	$\frac{1}{16}(\omega/U^2)$	$\frac{1}{8}(\omega/U^2)\cos(2\omega^{\frac{5}{2}}x/U^{\frac{7}{2}})$
J_{pf}	$-\frac{1}{8}(U/\omega)^{\frac{1}{2}}$	$\frac{1}{8}(U/\omega)^{\frac{1}{2}}$	$\frac{3}{8}(\omega/U^2)\cos(2\omega^{\frac{5}{2}}x/U^{\frac{7}{2}})$
J_p	$\frac{1}{4}(\omega/U^2)$	$\frac{1}{4}(\omega/U^2)$	$-\frac{1}{2}(\omega/U^2)\cos(2\omega^{\frac{5}{2}}x/U^{\frac{7}{2}})$
J	$-\frac{1}{8}(U/\omega)^{\frac{1}{2}}$	$\frac{1}{8}(U/\omega)^{\frac{1}{2}}$	0
(iii) $\omega_p \ll \omega$			
J_f	—	$\frac{1}{100}(1/\omega^{\frac{1}{5}})$	—
J_{pf}	—	$\frac{1}{50}(U/\omega^{\frac{4}{5}})$	—
J_p	—	$\frac{1}{25}(1/\omega^{\frac{1}{5}})$	—
J	—	$\frac{1}{20}(1/\omega^{\frac{1}{5}})$	

	upstream		
energy flux term:	k_3^+	k_3^-	cross term
(i) $\omega \ll \omega_p$			
J_f	$\frac{1}{36}(\omega/U^2)$	$-\frac{1}{36}(\omega/U^2)$	$-\frac{1}{27}(\omega/U^2)(\omega/U^{\frac{5}{3}})\cos(2U^{\frac{8}{3}}x)$
J_{pf}	$-\frac{1}{18}(\omega/U^2)$	$\frac{1}{18}(\omega/U^2)$	$-\frac{1}{9}(\omega/U^2)(\omega/U^{\frac{5}{3}})\cos(2U^{\frac{8}{3}}x)$
J_p	$\frac{1}{9}(\omega/U^2)$	$-\frac{1}{9}(\omega/U^2)$	$\frac{4}{27}(\omega/U^2)(\omega/U^{\frac{5}{3}})\cos(2U^{\frac{8}{3}}x)$
J	$\frac{1}{12}(\omega/U^2)$	$-\frac{1}{12}(\omega/U^2)$	0
(ii) $\omega_p \ll \omega$			
J_f	—	$-\frac{1}{100}(1/\omega^{\frac{1}{5}})$	—
J_{pf}	—	$\frac{1}{50}(U/\omega^{\frac{4}{5}})$	—
J_p	—	$-\frac{1}{25}(1/\omega^{\frac{1}{5}})$	—
J	—	$-\frac{1}{20}(1/\omega^{\frac{1}{5}})$	—

Transport of energy in this frequency range is, however, entirely due to the interaction between the two waves. The two large fluxes are $J_f(k_1^+, k_2^+)$ and $J_{pf}(k_1^+, k_2^+)$ with $J_p(k_1^+, k_2^+)$ small. It is significant that both $J_p(k_1^+, k_2^+)$ and $J_{pf}(k_1^+, k_2^+)$ are negative, indicating that the energy is travelling upstream towards the driver. The total flux is negative also.

The overall position, then, is that, for $\omega < \omega_s$ there exist two unstable downstream travelling waves, one exponentially large and one exponentially small. Both waves have zero total flux and any transport of energy is due solely to their interaction. The interaction leads to an upstream 'surge' of energy, which clearly will not be masked by the instabilities as suggested by Brazier-Smith & Scott. The total interaction flux is small and we have in fact already seen its effect. Figure 4 indicates that for $\omega < \omega_s$, $\mathrm{Re}\, A_0$ is negative, and that the driver is receiving and absorbing energy. This result must be due in part to the negative value of $J(k_1^+, k_2^+)$.

For $\omega_s < \omega < \omega_p$ the two downstream waves are neutral travelling waves. The fluxes associated with the wave $e^{ik_2^+ x}$ are all positive, and the energy and wave are right travelling. The fluid–plate flux is the largest in magnitude for both waves and

$J_{pf}(k_1^+)$ is negative. This term dominates the others and $J(k_1^+)$ is negative also. Hence the stable right-running wave has left-travelling energy. The group velocity of both waves is positive and using equation (5.14) we classify $e^{ik_1^+x}$ as a NEW and $e^{ik_2^+x}$ as a PEW.

For $\omega_p < \omega$, the only wave present is $e^{ik_2^+x}$. All fluxes are positive, and the large fluxes are J_p and J_f with the coupled fluid–plate flux no longer significant.

Upstream we find that, for $\omega < \omega_p$, all fluxes are of the same order and that J_p and J_f always have the same direction, which is that of the wave. The flux J_{pf} takes the opposite direction to the wave. The wavenumber k_3^+ generates a stable right-running wave with positive total flux. The energy in this wave is carried towards the drive point. Wavenumber k_3^- generates a stable left-running wave, with negative total flux, indicating left travelling energy. Both waves have negative group velocity and thus k_3^+ generates a NEW and k_3^- generates a PEW.

For $\omega_p < \omega$ there exists a stable left-running wave $e^{ik_3^-x}$ and the total flux of energy is left travelling.

6. Conclusions

In this paper we have examined the fundamental problem of structural acoustics in the presence of mean flow: the problem of determining the structure and fluid response when the structure is excited by localized forcing. We have concentrated on the low-frequency low-velocity régime in which mean flow effects are most pronounced, and for this régime have obtained asymptotic expressions for the significant characteristics of the waves generated by concentrated forcing of a thin elastic plate. The absolute instability boundary $U = U_c$ has been obtained exactly, and for all $U < U_c$ the response of the system has been obtained asymptotically in the convectively unstable frequency range $\omega < \omega_s(U)$, the anomalous neutral propagation range $\omega_s(U) < \omega < \omega_p(U)$, and the conventional neutral range $\omega > \omega_p(U)$. An exact energy equation for the system has been derived, and the way in which energy is transported through the system has been shown for convectively unstable and neutral waves.

The significant features of the study seem to us to be the following.

1. The characteristics of the waves generated upstream and downstream of the excitation are far from obvious, and can be settled by nothing less than the full implementation of the causality requirement for the correct interpretation of the Fourier integral for the response. This holds not only for $0 < \omega < \omega_s(U)$ where an incorrect interpretation of that integral would give, for example, a field in $x < 0$ and decaying exponentially there rather than an instability in $x > 0$ amplifying exponentially there. In the range $\omega_s(U) < \omega < \omega_p(U)$ we find a neutral wave mode which has group velocity directed towards the excitation. Such a situation would be forbidden by a group velocity radiation condition, but is permitted here, we argue, because the exciting force is not the sole source of wave energy (which would then radiate away at the group velocity) but also has a role as a scatterer. The imposition of a time-harmonic local constraint can convert steady mean flow energy into wave energy at the prescribed frequency, and the group velocity and the energy flux of the wave energy created in this way must be determined from the causality prescription, and not from use of a radiation condition.

2. Related to the above is the fact that $\mathrm{Re}\, A_0 < 0$ throughout $0 < \omega < \omega_s$ *and* $\omega_s < \omega < \omega_p$; and in fact $\mathrm{Re}\, A_0 \to -\infty$ as ω approaches ω_p from below. Thus to maintain the postulated fixed force excitation the external agency must be prepared

Table 4. *Summary of results for the phase velocities, group velocities, fluxes upstream and downstream of the excitation, and for the energy input at the drive point*

	(*a*) $\omega < \omega_s, U < U_c$	
one neutral NEW (k_3^+) → phase velocity ← group velocity → flux		one exponentially growing wave (k_2^+) → phase velocity → group velocity flux = 0[a]
one neutral PEW (k_3^-) ← phase velocity ← group velocity ← flux	↓ energy out $\mathrm{Re}\, A_0 < 0$	one exponentially decaying wave (k_1^+) → phase velocity → group velocity flux = 0[a]
	(*b*) $\omega_s < \omega < \omega_b, U < U_c$	
one neutral NEW (k_3^+) → phase velocity ← group velocity → flux		one neutral NEW (k_2^+) → phase velocity ← group velocity → flux
one neutral PEW (k_3^-) ← phase velocity ← group velocity ← flux	↓ energy out $\mathrm{Re}\, A_0 < 0$	one neutral NEW (k_1^+) → phase velocity → group velocity ← flux
	(*c*) $\omega_b < \omega < \omega_p, U < U_c$	
one neutral NEW (k_3^+) → phase velocity ← group velocity → flux		one neutral PEW (k_2^+) → phase velocity → group velocity → flux
one neutral PEW (k_3^-) ← phase velocity ← group velocity ← flux	↓ energy out $\mathrm{Re}\, A_0 < 0$	one neutral NEW (k_1^+) → phase velocity → group velocity ← flux
	(*d*) $\omega_p < \omega, U < U_c$	
one neutral PEW (k_3^-) ← phase velocity ← group velocity ← flux		one neutral PEW (k_2^+) → phase velocity → group velocity → flux
evanescent wave (k_3^+) of no far-field significance ← phase velocity	↑ energy in $\mathrm{Re}\, A_0 > 0$	evanescent wave (k_1^+) of no far-field significance → phase velocity

[a] There is a non-zero flux in the positive x-direction from the interaction between the two downstream waves.

to absorb wave energy at frequency ω: and indeed at a very large rate for ω just less than ω_p. Only for $\omega > \omega_p$ is the power flow from the drive into the system, and then the effects of mean flow are confined to minor perturbations of the much-studied problems of the fluid loading of static elastic structures. The directions of the phase and group velocities, of the energy flux and of the energy input are all summarized diagrammatically in table 4.

These features illustrate the profound effects that can follow the introduction of

mean flow, and we stress again that they arise not only where convective instabilities are found, but in the anomalous neutral frequency range also; indeed the largest effects occur at the boundary $\omega = \omega_p$ between the anomalous neutral range and the conventional neutral range. The whole pattern of energy flow into the wave fields in the fluid and the structure has been dramatically changed by the possibility of substantial conversion of mean flow energy to wave energy.

There is also a serious technical implication here. The whole character of the solution to a fixed-frequency excitation problem can be resolved only by carrying through the causality calculations, which are global and refer to frequencies of all magnitude. Such calculations, necessarily a mixture of numerical and asymptotics even in the simplest possible case, as here, pose severe technical problems for which there appear from the present work to be no short cuts.

This work has been carried out under support from the U.S. Office of Naval Research, code 1132SM (Dr Phillip Abraham).

Appendix. Exact evaluation of $\Psi(0)$

Evaluating (3.3) at the point of excitation ($x = 0$) we write

$$\Psi(0,\omega) = \int_{c_-(\omega)} \frac{k}{P_-(k,\omega)}\,\mathrm{d}k + \int_{c_+(\omega)} \frac{k}{P_+(k,\omega)}\,\mathrm{d}k. \tag{A 1}$$

We may close the contour in the upper half-plane (as in figure 3), or in the lower (using an appropriate similar path). It is evident that with $x = 0$, however, the branch line integrals give a contribution which is significant and must be evaluated.

Using Cauchy's Theorem we evaluate $\Psi(0)$, when closure takes place in the upper and lower half-planes respectively, as

$$\Psi(0,\omega) = 2\pi\mathrm{i}\sum_1^2 \frac{k_n^+}{P_+(k_n^+,\omega)} - \int_{\cup\!\!\!\uparrow} f(k)\,\mathrm{d}k, \tag{A 2}$$

$$\Psi(0,\omega) = -2\pi\mathrm{i}\left\{\frac{k_3^+}{P_+(k_3^+,\omega)} + \frac{k_3^-}{P_+(k_3^-,\omega)}\right\} - \int_{\cap\!\!\!\uparrow} f(k)\,\mathrm{d}k. \tag{A 3}$$

Here $\cup\!\!\!\uparrow$ and $\cap\!\!\!\uparrow$ represent integration around the branch cuts in the upper and lower half-planes respectively. Considering the branch line integrals, we now make a change of variables; let $k = \mathrm{i}v$ in (A 2) and $k = -\mathrm{i}v$ in (A 3). The paths of integration have now been moved to the real line, and

$$\int_{\cup\!\!\!\uparrow} f(k)\,\mathrm{d}k = \int_0^\infty \frac{v\,\mathrm{d}v}{P_+(\mathrm{i}v)} - \int_0^\infty \frac{v\,\mathrm{d}v}{P_-(\mathrm{i}v)}, \tag{A 4}$$

$$\int_{\cap\!\!\!\uparrow} f(k)\,\mathrm{d}k = \int_0^\infty \frac{v\,\mathrm{d}v}{P_+(-\mathrm{i}v)} - \int_0^\infty \frac{v\,\mathrm{d}v}{P_-(-\mathrm{i}v)}. \tag{A 5}$$

It is easily established from the definitions of $P_\pm$ (equation (2.13)), that $P_\pm(\bar{\alpha}) =$

$\overline{P_{\pm}(\alpha)}$, where overbar denotes complex conjugate. The sum of (A 4) and (A 5) can then be written as

$$\int_0^\infty \frac{v}{|P_+(\mathrm{i}v)|^2}[P_+(\mathrm{i}v)+\overline{P_+(\mathrm{i}v)}]\,\mathrm{d}v-\int_0^\infty \frac{v}{|P_-(\mathrm{i}v)|^2}[P_-(\mathrm{i}v)+\overline{P_-(\mathrm{i}v)}]\,\mathrm{d}v = 2B_0, \qquad \text{(A 6)}$$

where B_0 is real.

Returning to equations (A 2) and (A 3), the function $\Psi(0,\omega)$ is determined as

$$\Psi(0,\omega) = \pi\mathrm{i}\left\{\frac{k_1^+}{P'_+(k_1^+)}+\frac{k_2^+}{P'_+(k_2^+)}-\frac{k_3^+}{P'_+(k_3^+)}-\frac{k_3^-}{P'_-(k_3^-)}\right\}+B_0. \qquad \text{(A 7)}$$

References

Benjamin, T. B. 1960 Effects of a flexible boundary on hydrodynamic stability. *J. Fluid Mech.* **9**, 513–532.

Benjamin, T. B. 1963 The threefold classification of unstable disturbances in flexible surfaces bounding inviscid flows. *J. Fluid Mech.* **16**, 436–450.

Brazier-Smith, P. R. & Scott, J. F. 1984 Stability of fluid flow in the presence of a compliant surface. *Wave Motion* **6**, 547–560.

Cairns, R. A. 1979 The role of negative energy waves in some instabilities of parallel flows. *J. Fluid Mech.* **92**, 1–14.

Carpenter, P. W. & Garrad, A. D. 1986 The hydrodynamic stability of flow over Kramer-type compliant surfaces. Part 2. Flow-induced surface instabilities. *J. Fluid Mech.* **170**, 199–232.

Cremer, L., Heckl, M. & Ungar, E. E. 1973 *Structure-borne sound*. Berlin: Springer-Verlag.

Crighton, D. G. 1989 The 1988 Rayleigh medal lecture: fluid-loading – the interaction between sound and vibration. *J. Sound Vib.* **133**, 1–27.

Drazin, P. G. & Reid, W. H. 1981 *Hydrodynamic stability*. Cambridge University Press.

Fahy, F. J. 1985 *Sound and structural vibration*. London: Academic Press.

Gad-el-Hak, M. 1986 Boundary layer interaction with compliant coatings: an overview. *Appl. Mech. Rev.* **39**, 511–523.

Huerre, P. & Monkewitz, P. A. 1985 Absolute and convective instabilities in free shear layers. *J. Fluid Mech.* **159**, 151–168.

Huerre, P. & Monkewitz, P. A. 1990 Local and global instabilities in spatially developing flows. *Ann. Rev. Fluid Mech.* **22**, 473–537.

Junger, M. C. & Feit, D. 1986 *Sound, structures and their interaction*, 2nd edn. Cambridge, Massachusetts: M.I.T. Press.

Kop'ev, V. F. & Leont'ev, E. A. 1985 Energy aspect of the acoustic instability of certain steady-state vortices. *Akust. Zh.* **31**, 348–352.

Landahl, M. T. 1962 On the stability of a laminar incompressible boundary layer over a flexible surface. *J. Fluid Mech.* **13**, 609–632.

Lighthill, M. J. 1960 Studies in magneto-hydrodynamic waves and other anisotropic wave motions. *Phil. Trans. R. Soc. Lond.* A **252**, 397–430.

Lighthill, J. 1978 *Waves in fluids*. Cambridge University Press.

Ostrovski, L. A., Rybak, S. A. & Tsimring, L. Sh. 1986 Negative energy waves in hydrodynamics. *Usp. Fiz. Nauk* **150**, 417–437.

Riley, J. J., Gad-el-Hak, M. & Metcalfe, R. W. 1988 Compliant coatings. *A. Rev. Fluid Mech.* **20**, 393–420.

Yeo, K. S. & Dowling, A. P. 1987 The stability of inviscid flows over passive compliant walls. *J. Fluid Mech.* **183**, 265–292.

Received 14 November 1990; accepted 17 January 1991

PHILOSOPHICAL TRANSACTIONS OF THE ROYAL SOCIETY A MATHEMATICAL, PHYSICAL & ENGINEERING SCIENCES